International Journal of Nanomedicine

Dovepress

open access to scientific and medical research

Open Access Full Text Article

ORIGINAL RESEARCH

Multiomic Profiling and Neuroprotective Bioactivity of *Salvia* Hairy Root-Derived Extracellular Vesicles in a Cellular Model of Parkinson's Disease

Vincenzo Vestuto[1,*], Marisa Conte[1,*], Mariapia Vietri[1,*], Francesca Mensitieri[2], Valentina Santoro[1,3], Anna Di Muro[1], Mariaevelina Alfieri[4], Maria Moros[5,6], Maria Rosaria Miranda[1,3], Chiara Amante[1], Matteo Delli Carri[1], Pietro Campiglia[1], Fabrizio Dal Piaz[2,7], Pasquale Del Gaudio[1], Nunziatina De Tommasi[1,3], Antonietta Leone[1], Ornella Moltedo[1], Giacomo Pepe[1,3], Elisa Cappetta[1], Alfredo Ambrosone[1]

[1]Department of Pharmacy, University of Salerno, Fisciano, 84084, Italy; [2]Department of Medicine, Surgery and Dentistry "Scuola Medica Salernitana", University of Salerno, Baronissi, 84081, Italy; [3]National Biodiversity Future Center (NBFC), Palermo, 90133, Italy; [4]Clinical Pathology, Santobono-Pausilipon Children's Hospital, AORN, Naples, 80122, Italy; [5]Instituto de Nanociencia y Materiales de Aragón (INMA), CSIC-Universidad de Zaragoza, Zaragoza, Spain; [6]Biomedical Research Networking Center in Bioengineering, Biomaterials and Nanomedicine (CIBER-BBN), Madrid, Spain; [7]Operative Unit of Clinical Pharmacology, University Hospital "San Giovanni di Dio e Ruggi d'Aragona", Salerno, 84131, Italy

*These authors contributed equally to this work

Correspondence: Alfredo Ambrosone; Elisa Cappetta, Department of Pharmacy, University of Salerno, Fisciano, 84084, Italy, Email aambrosone@unisa.it; ecappetta@unisa.it

Purpose: Extracellular vesicles (EVs) are promising tools for nanomedicine and nanobiotechnology. The purification of mammalian-derived EVs involves intensive processes, and their therapeutic application raises multiple safety and regulatory issues. Plants have the potential to serve as nonconventional sources of therapeutically relevant EVs. In this context, we recently identified hairy roots (HRs) of medicinal plants as a novel biotechnological platform to produce EVs for human health.

Methods: Herein, we report the purification, omics profiling, and bioactivity of EVs isolated from HRs of the medicinal plants *S. sclarea* and *S. dominica*. EVs were isolated from conditioned media of HR cultures using differential ultracentrifugation (dUC) and size exclusion chromatography (SEC). The isolated EVs were characterized by nanoparticle tracking analysis (NTA) and electron microscopy. The proteomic and metabolomic profiles of the EVs were determined using mass spectrometry. Uptake studies and bioactivity assays, including confocal microscopy, MTT, flow cytometry, ROS quantification, and untargeted metabolomics analyses, were conducted in SH-SY5Y cells treated with the neurotoxin 6-hydroxydopamine (6-OHDA) to evaluate the therapeutic potential of EVs in an in vitro model of Parkinson's disease.

Results: *S. sclarea* HRs released nanosized round-shaped EVs with a distinctive molecular signature. HR EVs from *S. sclarea* and *S. dominica* revealed conserved cargo of secondary metabolites, predominantly triterpenoids, which are known for their antioxidant properties. We showed that HR EVs are safe, enter the cells, and strongly inhibit apoptosis in a cellular model of Parkinson's disease. Cellular metabolomics revealed that EVs preserved metabolic homeostasis and mitigated cellular oxidative stress when co-administered with 6-OHDA. Mechanistically, HR EVs inhibited 6-OHDA autoxidation and substantially reduced the accumulation of its oxidative products, which are responsible for 6-OHDA-induced toxicity.

Conclusion: Collectively, our findings provide compelling evidence that EVs isolated from the hairy roots of *Salvia* species are promising, non-mammalian alternative for the design of novel therapies targeting neurological disorders.

Keywords: non-mammalian EV source, *Salvia* extracellular vesicles, hairy roots, nanomedicine, neuroprotection, Parkinson's disease

Introduction

Extracellular vesicles (EVs) are membrane-enclosed, non-replicating nano- to micro-sized particles naturally secreted by cells in diverse physiological and pathological contexts.[1,2] By transporting proteins, lipids, nucleic acids, and metabolites,

Received: 26 June 2024
Accepted: 3 September 2024
Published: 11 September 2024

Graphical Abstract

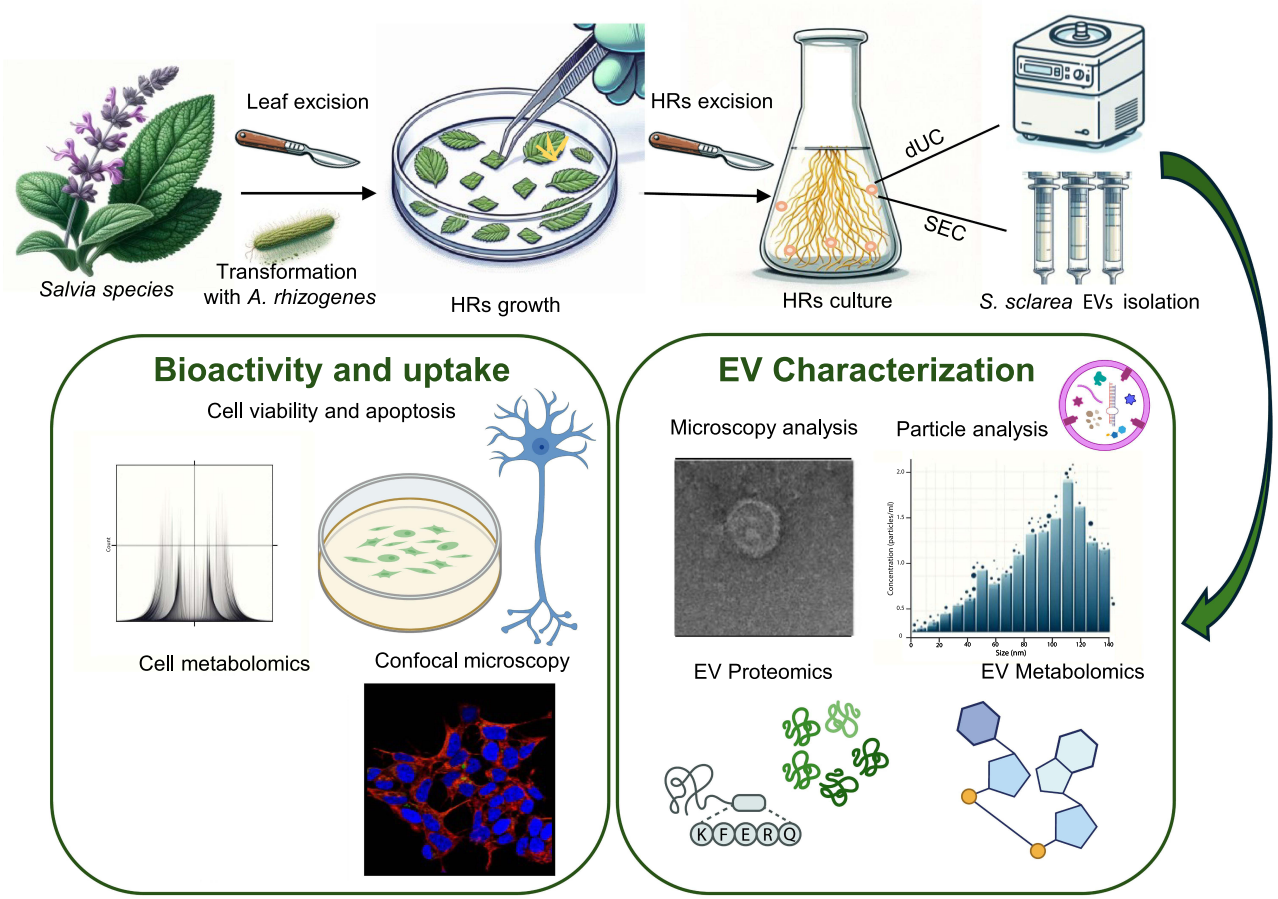

EVs drive molecular information exchange, shaping the biological processes of recipient cells and generating a global network of intercellular communications that connects organisms across species and kingdoms.[3–5]

From a pharmaceutical perspective, EVs could represent next-generation nanocarriers with an innate capability to penetrate biological barriers, associated with good biocompatibility and the possibility of targeting specific cells.[6,7] Nonetheless, isolating EVs from mammalian systems poses several challenges, including resource-intensive purification methods and consequent high production costs. This may hinder the large-scale manufacturing and integration of these nanocarriers into healthcare systems, thereby limiting their broader adoption in medical applications. Additional health concerns have been raised, such as immunogenicity and potential disease transmission linked to the cargo of mammalian EVs inherited from their parent cells, as reported for the seeding of toxic amyloid beta species in recipient neurons[8] or the delivery of long non-coding RNAs involved in carcinogenesis.[9] To bypass these potential risks, rigorous screening of biological sources, standardized procedures for EV purification/characterization and quality control measures are needed to maximize the reproducibility of EV preparations and mitigate any potential hazards. Currently, the EV research community is actively exploring non-conventional sources of EVs as viable alternatives to those derived from mammals for nanomedicine applications.[10]

Recently, plant-derived nano-and microvesicles (PDVs) have emerged as promising candidates for this purpose. Owing to their various molecular biocargos, including subsets of lipids, proteins, small non-coding RNAs (sncRNAs), and metabolites, PDVs exhibit a multitude of biological properties, such as antioxidant, antimicrobial, anti-inflammatory, anticancer, and wound-healing activities.[11,12] Although these results hold clinical promise, it is important to note that PDVs are typically extracted from plant tissues and organs through destructive methods. Consequently, preparations often include a mix of EVs and other vesicles, including intracellular and artificially created nano- and microvesicles. Additionally, EV isolation from

fresh fruits and vegetables does not permit standardization of EV preparations, which can significantly differ between batches owing to intraspecific genetic diversity, seasonality, plant treatments, soil chemical composition, and geographical origins.

Plant biotechnology tools, especially cell and tissue cultures, could overcome these limitations and represent a promising direction for future plant EVs research.[13] In this scenario, we have extensively focused our studies on the use of hairy roots (HRs) as a biofactory to produce plant EVs and to assess their biomedical exploitation.[14] HRs represent a fascinating biotechnological system involving the interaction between a soil bacterium, specifically *Agrobacterium rhizogenes*, and plants. During this interaction, *A. rhizogenes* transfers a fragment of DNA (T-DNA) into the plant genome, causing a hormonal imbalance that ultimately leads to the growth of ectopic roots, which can be excised and cultured in vitro.[15] Nowadays, HRs are adopted as versatile sources of valuable secondary metabolites with a consolidated use in pharmaceutics, cosmetics and nutraceutics. HRs may also enhance EV production, encompassing enhanced quality, sterility, and absence of harmful contaminants. Furthermore, HRs offer scalability required for industrial production and extensive applications.[16,17]

Our group recently demonstrated that EVs isolated from the conditioned media of *Salvia dominica* HRs have selective pro-apoptotic activity in pancreatic and breast cancer cell lines. We also provided compelling evidence that HRs allow consistent purification of EVs, safeguarding their intrinsic biomolecular content and reproducible bioactivity.[14]

Here, we expanded our knowledge of the use of plant HRs as a non-conventional source of EVs and their potential therapeutic applications in Parkinson's disease (PD). We conducted a comprehensive biophysical and biomolecular analysis of EVs extracted from the conditioned media of two medicinal plants, *Salvia sclarea* and *Salvia dominica*. This analysis includes the generation of extensive EV proteomic and metabolomic datasets. In an in vitro cellular PD model using 6-hydroxydopamine (6-OHDA) to simulate oxidative stress and neurodegeneration in neuroblastoma SH-SY5Y cells, we found that HR EVs exhibited significant pharmacological properties. In conclusion, our findings demonstrate that the HRs of *Salvia spp*. are reliable, non-conventional sources of EVs capable of neutralizing the toxic effects induced by 6-OHDA administration, thereby holding promise for their application in treating Parkinson's disease.

Materials and Methods

Hairy Roots Production

In this study, we used EVs freshly isolated from *Salvia sclarea* L., and *Salvia dominica* L. hairy roots. *Salvia dominica* HRs generation and characterization were broadly described in our previous study.[14] *S. sclarea* seeds (Lot. # 2494) were purchased from B&T World Seeds, France. The fruits "nutlets" of *S. dominica* were collected in May 2022 at As-Subayhi, in the Balqa Governorate, 20 km northwest of As-Salt City, Jordan, and identified by Prof. Ammar Bader. A voucher specimen number JO/IT-2022/1 has been deposited in the Herbarium of Laboratory of Pharmacognosy at Umm Al-Qura University, Makkah, Saudi Arabia. To produce *S. sclarea* HRs, seeds were surface sterilized using a 70% ethanol solution for 2 min. After ethanol elimination, the seeds were transferred to a 10% sodium hypochlorite solution for 10 min. To eliminate residual bleach, seeds were washed with sterile water. Following sterilization, the seeds were sown in MS 30 medium containing 4.30 g/L Murashige and Skoog (MS) salts including vitamins (Duchefa Biochemie, Haarlem, Netherlands),supplemented with sucrose (30 g/L), microagar (9 g/L), . The final pH of the medium was adjusted to 5.8. The seedlings were then placed in a growth chamber maintained at 23 °C. The photoperiod was set to 8 h in the dark followed by 16 h of light (130 µmol m^{-2} s^{-1}). To generate HRs, leaf explants of 20-day-old *S. sclarea* plants were transformed using *Agrobacterium rhizogenes* (ATCC® 15834). The explants were then dried, sterilized, and transferred onto an antibiotic-free MS 30 solid medium for 3 d at 26 °C. To eradicate *A. rhizogenes*, the explants were transferred to fresh MS 30 medium containing cefotaxime (100 mg/L) and kept in the dark at 23 °C. Weekly transfers to new medium with cefotaxime were performed for three weeks, with a reduction in antibiotic concentration to 50 mg/L. Healthy and differentiated hairy roots were excised, cultured individually on solid medium with cefotaxime (100 mg/L), and then transferred to hormone-free MS 30 liquid medium in 250 mL sterile glass jars with cefotaxime (50 mg/L). Both HR cultures were maintained in an incubator at 28 °C and with agitation (120 rpm).

Isolation of EVs from Hairy Roots-Conditioned Media

HR EVs were isolated from conditioned media of *S. sclarea* and *S. dominica* HRs using two widely used purification methods: Differential Ultracentrifugation (dUC) and Size Exclusion Chromatography (SEC).

Differential Centrifugation

The dUC purification protocol involved two initial low-speed centrifugations, first at 500 × *g* for 10 min at 4 °C and then at 2,000 × *g* for 20 min at 4 °C, to remove cells released from the roots in the culture medium. The supernatants were then filtered using 0.45 µm pore size membrane filters (Merck Millipore) to eliminate cellular debris and organelles. The filtered solution was then transferred to 50 mL Beckman polypropylene tubes and centrifuged with a Beckman Type 70 Ti fixed-angle titanium rotor (k-factor: 44) at 15,000 × *g* for 20 min to remove microvesicles, which typically have a diameter greater than 300–500 nm. The supernatant was transferred to new polycarbonate tubes (Beckman Coulter, No. 355631) in a Beckman Coulter Optima™ L-90K and ultracentrifuged at 100,000 × *g* for 3 h with a Type 70 Ti rotor to isolate extracellular vesicles of expected sizes between 50–200 nm. The obtained pellet was resuspended in 30–60 microliters of MilliQ water and stored at −80 °C for subsequent biophysical analyses.

Size Exclusion Chromatography

Size exclusion chromatography (SEC) was used to isolate EVs from the conditioned media of HRs. First, the HR growth medium was centrifuged at a low speed to remove cell debris, and the supernatant was filtered using 0.45 µm filters. The eluate was separated using Izon's qEV size-exclusion chromatography columns (Gen 2 qEV), and the EVs were eluted from the column filler with PBS according to the manufacturer's instructions. EV preparations were stored at −80 °C for subsequent biophysical and bioactivity analyses. SEC purification was conducted in a laminar hood to maintain sterility.

Characterization of HR EVs

Sodium Dodecyl Sulfate Polyacrylamide Gel Electrophoresis (SDS-PAGE) and Silver Staining

Ten microliters of *S. sclarea* HR EVs, purified as described in Section 2.2, were resolved by SDS-PAGE (10% polyacrylamide gel). The gel was then silver-stained as previously described for *S. dominica*.[14]

Determination of EV Size and Concentration – Nanoparticle Tracking Analysis (NTA)

Size distribution and concentration of *Salvia spp*. HR EVs were determined by Nanoparticle Tracking Analysis (NTA) using a NanoSight NS300 instrument (Malvern Instruments, Malvern, UK) equipped with a green laser and sCMOS camera. The samples were diluted 1:100 in Milli-Q water to obtain 20 number of particles per frame and were injected into the laser chamber for analysis. Data acquisition was performed using the following settings: camera level 15, acquisition time, 60s; detection threshold, 4. Three videos were recorded under RT and flow conditions at a syringe speed of 30 infusion rates. Subsequently, the videos were analyzed using NanoSight NTA 3.4 software to perform tracking analysis. All measurements were performed in biological triplicates.

Scanning Electron Microscopy (SEM)

Ten microliters of *S. sclarea* and *S. dominica* HR EV (10^{10} particles/mL) were diluted and fixed with 10 µL of a 4% paraformaldehyde solution and then maintained at 4 °C for a minimum of two hours. A suspension of this fixed preparation (5 µL) was applied to the carbon-coated electron microscopy stubs. Subsequently, the samples were dried using a nitrogen flux under a chemical fume hood. SEM images of the samples were captured using a Tescan Solaris instrument (Tescan Orsay Holding, Brno, Czech Republic). Analyses were carried out at 1.5 and 5.0 keV without applying any coating to the particles. SEM imaging was performed on EVs obtained from three distinct preparations.

Transmission Electron Microscopy (TEM)

Before using a grid of carbon film supported on a 300 mesh copper grid, a glow discharge was performed on it (30s 15mA). Ten microliters of *S. sclarea* HR EVs (10^{10} particles/mL) were fixed using glutaraldehyde 2.5% in PBS and deposited on a parafilm. The grid was placed on the drop for 5 min, washed with distilled water for 1 min, and placed for 1 min in a drop of 3 mL of 2% staining agent (Methylamine Vanadate, NanoVan) diluted in H_2O before washing it with water for 1 min. TEM images were collected using a FEI Tecnai T20 (FEI Europe, Eindhoven, Netherlands) at the Laboratorio de Microscopias Avanzadas (Universidad de Zaragoza, Spain).

Assessment of *A. rhizogenes* Contamination

To confirm the absence of *A. rhizogenes* contamination in the EV preparations, we conducted Polymerase Chain Reactions (PCR) using 5 µL HR EV preparations as templates. Bacterial genes (*rolB, rolC* and *VirD2*) were detected using the Phire Plant Direct PCR Kit (Thermo Fisher Scientific Inc., Darmstadt, Germany) with the specific primers listed Table S1. The *A. rhizogenes* pRi15834 plasmid was extracted using the QIAprep® Spin Miniprep Kit (Qiagen, Hilden, Germany) and used as a positive control for PCR. DNA amplification was carried out under the following conditions: initial denaturation at 95 °C for 5 min, followed by 35 cycles of denaturation at 95 °C for 30s, annealing at 55 °C for 30 min, extension at 72 °C for 1 min, and a final extension at 72 °C for 5 min. Subsequently, the PCR-amplified products were analyzed on a 1% agarose gel.

Proteomic Profiling and Bioinformatic Analysis

Protein extracts from purified *S. sclarea* hairy roots (30 µg) and 50 µL of dUC-purified *S. sclarea* HR EVs (10^{10} particles/mL) were separated by 12% SDS-PAGE. The gels were then sectioned into 10 pieces and each sample underwent a trypsin in gel digestion procedure. The obtained peptide mixtures were analyzed using an Orbitrap Q-Exactive Classic Mass Spectrometer (Thermo Fisher Scientific Inc., Darmstadt, Germany) coupled with a nanoUltimate300 UHPLC system (Thermo Fischer Scientific). Peptide separation was conducted on a capillary EASY-Spray PepMap column (0.075mmÅ~ 50 mm, 2 µm, Thermo Fisher Scientific) employing aqueous 0.1% formic acid (A) and CH_3CN containing 0.1% formic acid (B) as mobile phases and a linear gradient from 3 to 40% of B in 45 min, and a 300 $nL \cdot min^{-1}$ flow rate. Mass spectra were acquired over an m/z range from 375 to 1500. To achieve sequence confirmation, MS and MS/MS data were analyzed using Mascot software (v2.5, Matrix Science) and the non-redundant Data Bank UniprotKB/Swiss-Prot (Release 2021_03), limited to green plant proteins (Viridiplantae). The parameter sets were trypsin cleavage, carbamidomethylation of cysteine as a fixed modification, methionine oxidation as a variable modification, a maximum of two missed cleavages, and false discovery rate (FDR), calculated by searching the decoy database at 0.05. Proteomic analyses were performed in duplicate on three different vesicle preparations and three *S. sclarea* HR extracts. Only proteins that were commonly identified in all the experiments were considered. Gene ontology analysis (Biological Process category) of identified proteins was carried out using the specific analysis tool ShinyGo 0.80 with a False Discovery Rate (FDR) cutoff of 0.05, taking into consideration only pathways involving more than two proteins.

To identify conserved EV markers, *Salvia sclarea* and *Salvia dominica* EV proteomes were compared and the 15 common proteins identified were compared with the apoplastic EV proteome of the model plant *Arabidopsis thaliana*, previously reported.[18] FASTA sequences for the 15 common EV-associated proteins identified in *Salvia sclarea* and *Salvia dominica* proteins were obtained from UniProt database and aligned with those from humans (genome assembly GRCh38.p14) using the blastp mode of BLAST on Ensembl (https://www.ensembl.org/index.html). An alignment was considered to predict a homologue if the identity of at least 50% within this region was observed. The complete Vesiclepedia database (downloaded and accessed on April 23, 2024) was imported into the FunRich version 3.1.3. The list of the top 100 proteins identified in EVs according to Vesiclepedia was obtained from ExoCarta (http://exocarta.org/) and compared with the human homologues identified.

Metabolomic Profiling of HR EVs

EV preparations (10^{10} particles/mL) obtained through dUC from conditioned media of *S. dominica* and *S. sclarea* HRs were subjected to Liquid Chromatography-Mass Spectrometry (LC-MS) to identify specialized metabolites. The analytical setup provides the used a Thermo Scientific UltiMate 3000 UHPLC system with a Luna® C_{18} 150×2 mm, 3 µm (100 Å) column (Phenomenex®, Castel Maggiore, Bologna, Italy) and as eluent acidified water with 0.1% formic acid (v/v) (solvent A) and acetonitrile (solvent B). The gradient used was as follows: a solvent B from 5 to 95% over 35 min. with a flow rate of 0.2 mL/min and a column oven at 30 °C. A Q Exactive™ Hybrid Quadrupole-Orbitrap™ Mass Spectrometer (Thermo Fisher Scientific Inc., Darmstadt, Germany) was used in negative and positive ion modes. Specialized metabolites were identified through accurate MS measurements by comparing both full and fragmented mass spectra against standard compounds and existing literature data. Sample preparation, experimental analysis, quality

control, metabolite identification, and data preprocessing were carried out according to the Metabolomics Standards Initiative.[19]

Bioactivity and Cellular Uptake of HR EVs

Cell Culture and Drug Treatment

The human neuroblastoma SH-SY5Y cell line was obtained from the American Type Culture Collection (ATCC, Rockville, MD, USA). Cells were grown in Dulbecco's Modified Eagle Medium (DMEM, 4500 mg/mL glucose) supplemented with 10% (*v*/*v*) fetal bovine serum (FBS), 2 mM L-glutamine, 100 U/mL penicillin, and 0.1 mg/mL streptomycin. Cells were routinely grown in culture dishes (Corning, Corning, NY) in an environment containing 5% CO_2 at 37 °C and split every two days. In each experiment, cells were placed in fresh medium, cultured in the presence of *S. sclarea* and *S. dominica* HR EVs, and co-administered with different concentrations of neurotoxic agents: 50–100 µM 6-OHDA (Sigma Aldrich, St. Louis, MO, USA), 1 µM mitoxantrone (Sigma Aldrich, St. Louis, MO, USA), 400 µM hydrogen peroxide (Sigma Aldrich, St. Louis, MO, USA), 40 µM amyloid β-peptide (1–42) (Anaspec, Campus Dr Fremont, CA, USA).

Cell Viability Assay

Cell viability was assessed by measuring mitochondrial metabolic activity with 3-[4,5-dimethylthiazol-2,5-diphenyl-2H-tetrazolium bromide (MTT).[20] In brief, SH-SY5Y cells (5×10^4 cells/well) were plated in 96-well plates for 24 h. Then, dUC-purified or SEC-purified *S. sclarea* and *S. dominica* HR EVs (10^8–10^4 vesicles) were added either alone or in combination with 6-OHDA (100 µM) for 24 h. Vehicle controls were obtained by adding MilliQ water and PBS for dUC- or SEC-purified EVs, respectively. Equal volumes of MS 30 culture medium and EV-depleted medium were used as additional experimental controls. More specifically, MS 30 medium was used as the non-conditioned medium for HRs. The EV-depleted medium was obtained by collecting the supernatant from the final centrifugation step at 100,000 × *g*. Then, 100 µL per well of 0.1 M isopropanol/HCl solution was added to dissolve the formazan crystals. The absorbance was measured at 570 nm using a microplate reader (Multiskan Go, Thermo Fisher Scientific). Cell viability was expressed as a percentage relative to the untreated cells cultured in a medium with 0.1% DMSO and set to 100%, whereas 10% DMSO was used as positive control and set to 0% of viability.

Fluorescent Labelling of EVs and Cell Uptake analysis by Confocal Microscopy

S. sclarea HR EVs were labelled using BODIPY® FL N-(2-aminoethyl)maleimide (Thermo Fisher Scientific, MA, USA), spectrally similar to negatively charged fluorescein dye. Briefly, 10 mM BODIPY dye was added during the purification procedure after centrifugation at 15,000 × *g* to label the enriched fraction of the small EVs. After 15 min of incubation at room temperature, EVs were precipitated at 100,000 × *g*. The supernatant (EV-depleted medium) was removed and used as a labelling control in the confocal analyses. To rinse out the excess of free BODIPY, the EV pellet was washed by resuspension in 30 mL MilliQ water. Subsequently, EVs were purified using dUC, as described above. Fluorescently labelled HR EVs were administered to SH-SY5Y cells (seeding density: 5×10^4 cells/well) previously seeded in 24-well on 12 mm round cover glasses. After 24 h, the cells were stained for immunofluorescence as previously reported.[21] Briefly, cells were extensively washed with PBS-Tween 20 (0.1%), fixed with 4% paraformaldehyde for 20 min, permeabilized in 0.1% Triton-X-100 in PBS for 10 min, and then blocked for 1h in blocking buffer (0.5% BSA in PBS-Tween 20). Following overnight incubation with TRITC-Phalloidin 2 µg/mL, the slides were washed with PBS-Tween 20 and nuclei were stained with 1 µg/mL 4.6-diamidino-2-phenylindole (DAPI) (Thermo Fisher Scientific). Images were finally acquired by using a Zeiss LSM 710 confocal microscope.

Apoptosis Analysis by Flow Cytometry

Hypodiploid nuclei were analyzed by flow cytometry using propidium iodide (PI) staining. SH-SY5Y cells (3×10^5 cells/well) were grown in 12-well plates and allowed to adhere for 24 h. Subsequently, the medium was replaced and the cells were treated with HR EVs (10^8 particles/mL) and 6-OHDA (50 µM) for 24 h. After treatment, the culture medium was replaced, cells were washed twice with PBS and then suspended in 300 µL of a hypotonic staining solution containing 50 µg/mL PI, 0.1% (*w*/*v*) sodium citrate, and 0.1% Triton X-100. The culture medium and PBS were centrifuged, and cell

pellets were pooled with cell suspensions to retain both dead and living cells for analysis. After incubation at 4 °C for 30 min in the dark, cell nuclei were analyzed with a Becton Dickinson FACScan flow cytometer using the Cell Quest software version 4 (Franklin Lakes, NJ, USA). Cellular debris were excluded from the analysis by raising the forward scatter threshold, and the percentage of cells in the hypodiploid region (sub G0/G1) was calculated.

Reactive Oxygen Species (ROS) Quantification

Intracellular reactive oxygen species (ROS) levels were measured using 10 μM 6-carboxy-2′,7′-dichlorodihydrofluorescein diacetate (DCFH-DA; Sigma Aldrich, St. Louis, MO, USA) as previously described.[22] To test the effects of *Salvia spp*. EVs on ROS neutralization, SH-SY5Y cells were seeded (5×10^4 cells/well) in 96-well plates and allowed to adhere for 24 h. The cells were then treated for 1 h with EVs (10^8 vesicles), 6-OHDA (100 μM), or a combined administration of both. After incubation, the medium was removed and the cells were washed twice with PBS. A staining solution containing DCFH-DA in serum-free medium without phenol-red was added for 30 min at 37 °C in the dark. Cells were detached manually, washed, centrifuged, and resuspended in a PBS/BSA (2% w/v) solution. Fluorescence signals were evaluated using a Becton Dickinson FACScan flow cytometer and analyzed using Cell Quest software, version 4 (Franklin Lakes, NJ, USA). A FSC-H (x-axis) Vs SSC-H (y-axis) plot was generated, and the cells were gated to exclude dead cells and debris.

RNA Extraction, Reverse-Transcription and Real-Time Quantitative Reverse Transcription PCR (qRT-PCR)

SH-SY5Y cells (5×10^5 cells/well) were plated into 6-well plates for 24 h, and then HR EVs (10^8 particles/mL) were added either alone or in co-administration with 6-OHDA (50 μM) for 24 h. Total RNA was isolated from the treated cells with TRIzol (Thermo Fisher Scientific, MA, USA), according to the manufacturer's instructions. The concentration and purity of RNA were determined spectrophotometrically by measuring the absorbance at 260/280 nm and 260/230 nm. RNA integrity was checked by 2% (w/v) agarose gel electrophoresis. One microgram of total RNA was treated with DNase I (Thermo Fisher Scientific) and reverse-transcribed using M-MLV Reverse Transcriptase using SuperScript III Reverse Transcriptase (Thermo Fisher Scientific) and random hexamers. Thermal conditions for reverse transcription were 25 °C for 10 min, 37 °C for 50 min, and 75 °C for 15 min. Gene expression analysis of *(PTEN)-induced putative kinase 1* (*PINK1*; NM_032409.3) and *Parkinson's disease 2* (*PARK2/parkin*; AB245403.1) was carried out by qRT-PCR in a QuantStudio 5 Real-Time PCR Instrument. Each PCR reaction consisted of 1 μL of 1:20 diluted cDNA, 5 μL of 2X PowerUp SYBR Green Master Mix (Applied Biosystems, CA, United States), and 0.4 μM of each gene-specific primer in a total volume of 10 μL. Thermal cycling included an initial cycle at 50 °C for 2 min and 95 °C for 2 min, followed by 40 cycles of denaturation at 95 °C for 15s, annealing at 56 °C for 15s, extension at 72 °C for 30s. Values were determined from standard curves generated from serial cDNA dilutions and normalized to *glyceraldehyde-3-phosphate dehydrogenase* (*GAPDH*; GenBank: AY340484.1). The primers used are listed in Table S1. Expression changes were calculated by the $2^{-\Delta\Delta CT}$ method.[23] Untreated cells were used as calibrator samples.

Metabolome Extraction and LC-MS/MS Analysis in Cells

The metabolites were extracted as follows: cell pellets were thawed on ice, and 300 μL of ice-cold MeOH/H_2O (80:20) were added, vortexed for 30s, and subjected to 10 min of sonication in sweep mode. The samples were then centrifuged at 14,680 rpm for 10 min at 4 °C and the upper layer was collected and evaporated using a SpeedVac™ (Savant™, Thermo Scientific™, Milan, Italy). Subsequently, the dried samples were solubilized in an ACN/H_2O solution (70:30) before injection into RP-UHPLC-ESI-HRMS.

Metabolome analyses were performed using a Vanquish™ UHPLC system coupled online with an Orbitrap Exploris™ 120 mass spectrometer (Thermo Scientific™, Bremen, Germany) equipped with a heated electrospray ionization probe (HESI II).

The separation was performed in reversed phase mode, with an ACQUITY UPLC™ HSS T3 Column (150 × 2.1 mm × 1.8 μm) (Waters Corp., Milford, MA, USA). The column temperature was set to 45 °C, and the flow rate was 0.3 mL/min. The mobile phase was (A): H_2O with 0.1% HCOOH (v/v) and (B): ACN with 0.1% HCOOH (v/v) for positive ionization mode and (A) H_2O + 1mM NH_3F and (B) ACN for analysis in negative ion mode. The following gradient was employed: 0.01–9.00 min, 0–98% B; 9.01–10.00 min, 98% B isocratic; 10.01–10.50 min, 98–

0% B; then five min for column re-equilibration. 3 µL were injected. All additives and mobile phases were of LCMS grade and purchased from Merck (Milan, Italy).

The MS was calibrated by Thermo calmix Pierce™ calibration solutions for both polarities. Full MS (70–800 m/z) and data-dependent MS/MS were performed at a resolution of 15,000 and normalized collision energy (NCE) values of 20, 40, and 60 were used. Source parameters were set as it follows: sheath gas pressure, 40 arbitrary units; auxiliary gas flow, 15 arbitrary units; spray voltage, +3.3 kV, −3.3 kV; capillary temperature, 280 °C; auxiliary gas heater temperature, 300 °C.

For data analysis, Compound Discoverer™ 3.1 software (Thermo Scientific) was used for raw data processing (baseline correction, noise filtering, spectral alignment, and peak detection) and tentative identification of metabolites based on molecular formula (matched), exact mass (mass tolerance of <2 ppm), and MS2 fragmentation pattern [Fragment Ion Search (FISh)], with a global database search (mzCloud, MassList, and ChemSpider). Statistical analysis was conducted using the online tool MetaboAnalyst 5.0 (https://www.metaboanalyst.ca/). During this phase, a sequential application of normalization by median, logarithmic transformation, and autoscaling was performed. The autoscaling step entailed centering at the mean and scaling by the standard deviation for each variable. For the subsequent enrichment analysis, the identified metabolites were correlated with the Human Metabolome Database (HMDB) and KEGG IDs. This analytical step was also performed using MetaboAnalyst, utilizing the KEGG pathway library associated with *Homo sapiens*.

6-OHDA Auto-Oxidation Assay

Auto-oxidation of 6-OHDA was evaluated spectrophotometrically by monitoring the formation of *p*-quinone at 490 nm, as previously reported[24] in a cell-free system under conditions corresponding to the cellular treatments reported above. DMEM without FBS containing *Salvia spp*. EVs (10^8 particles/mL) in a 96-well plate were thermostatically maintained at 37 °C during the experiment. NAC (1 mM) was used as positive control. The experiment was initiated by the addition of 6-OHDA to give a final concentration of 175 µM. Absorbance at 490 nm was monitored at 1h intervals for 8h.

Melanin Formation Assay

Melanin formation was evaluated spectrophotometrically at 405 nm in a cell-free system as previously reported.[25] 6-OHDA was incubated with or without $FeSO_4$ (300 µM) and *Salvia spp*. EVs (10^8 particles/mL) in DMEM without FBS in a 96-well plate thermostatically maintained at 37 °C during the experiment. After incubation for various periods at 37 °C, the absorbance was measured at 405 nm. The experiment was initiated by adding 6-OHDA at a final concentration of 100 µM. Absorbance at 405 nm was monitored at 1h intervals for 8h.

Statistics and Reproducibility

The sample size and number of replicates for each experiment are reported in the figure legends, where possible. Otherwise, these data were properly reported throughout the materials and methods section. Data are reported as mean ± standard deviation (SD) of results from at least three independent experiments. Analysis of variance (ANOVA) and multiple comparisons with the Bonferroni's test employed to assess HR EV effects were carried out with GraphPad Prism 8.0 software (San Diego, CA, USA). *P*-values ≤0.05 (*), ≤0.01 (**) and ≤0.001 (***) were considered to be statistically significant.

Results

Hairy Roots are Reliable Biotechnological Sources of Non-Mammalian EVs

In this work, EVs were purified from the HRs of two medicinal plants, *Salvia dominica* and *Salvia sclarea*. Full characterization of *S. dominica* HRs was previously reported by our group,[14] whereas we report, for the first time, the purification and characterization of EVs derived from the conditioned medium of *Salvia sclarea* HRs. These HRs were obtained according to standard procedures by infecting *S. sclarea* leaf explants with a hypervirulent strain of *Agrobacterium rhizogenes* (ATCC 15834), as schematically illustrated in Figure 1A. Stable and *A. rhizogenes*-free HRs were then transferred to liquid medium and cultured for up to two months. Conditioned media of HRs were collected weekly for EV purification using differential ultracentrifugation (dUC) and size exclusion chromatography (SEC) (Figure 1B).

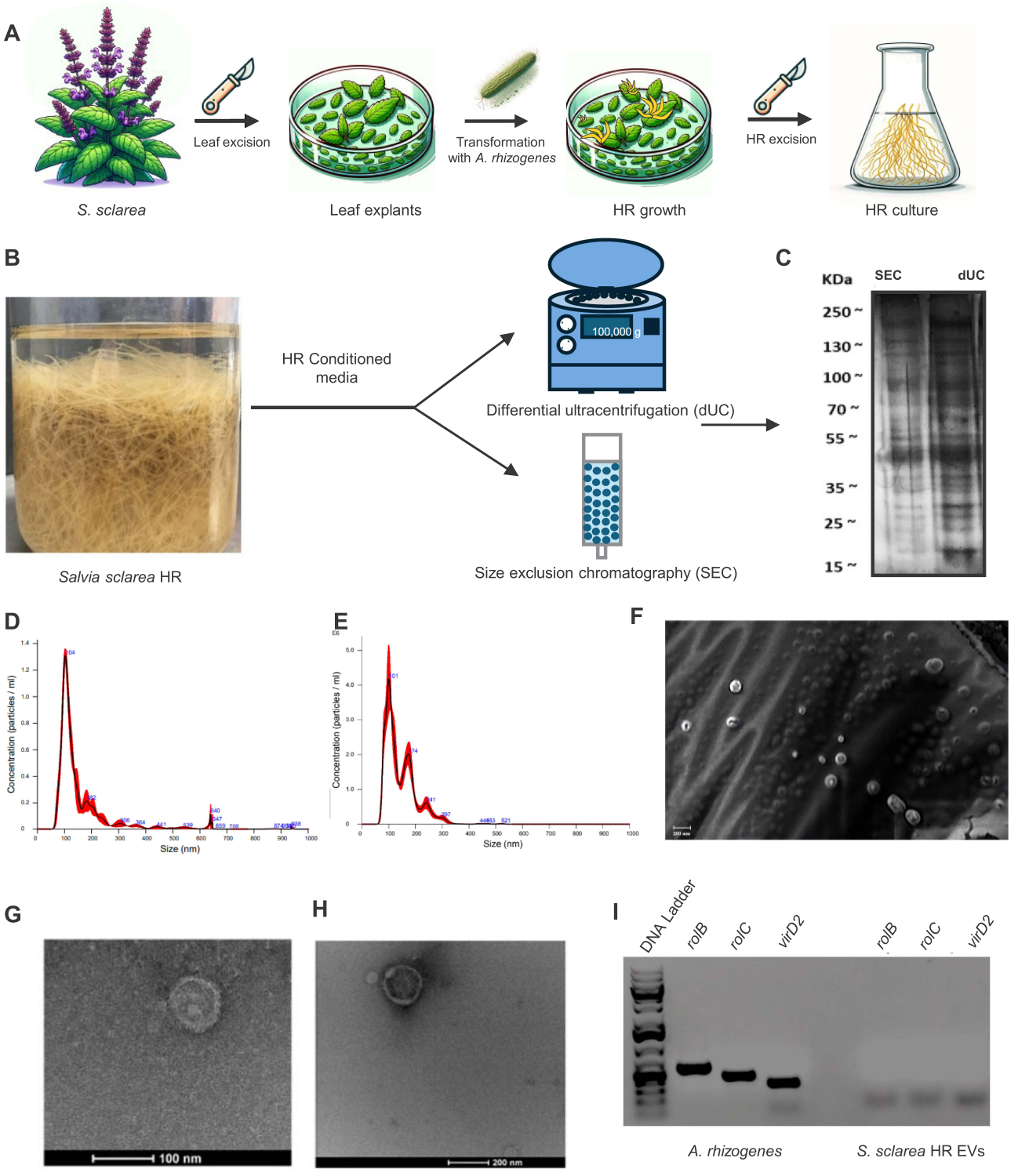

Figure 1 Isolation and characterization of EVs from *Salvia sclarea* HR conditioned medium. (**A**) Representative image of *S. sclarea* HR culture employed as EV biofactory. (**B**) Conditioned media were collected from two-month-old HRs and used for the purification of EVs by differential ultracentrifugation (dUC) or size exclusion chromatography (SEC). (**C**) Protein profile analysis of HR-derived EVs visualized through SDS-PAGE and silver staining. (**D** and **E**) Nanoparticle Tracking Analysis (NTA) measurements depict the size distribution of *S. sclarea* HR EVs purified by dUC (dilution= 1: 100) and SEC (dilution= 1:5), respectively. (**F**) Scanning electron image showing a group of *S. sclarea* HR EVs. (**G**) and (**H**) Transmission electron microscopy (TEM) close-up images displaying the round-shaped morphology of *S. sclarea* HR EVs. (**I**) Amplification of *rolB, rolC* and *virD2* genes, located in the pRi15834 agrobacterium-type Ri plasmid was carried out through PCR in HR EVs. pRi15834 plasmid extracted from *A. rhizogenes* was employed as template for positive PCR control. Scale bars: 200 nm in (**F**), 100 nm in (**G**), 200 nm in (**H**).

SDS-PAGE and silver staining of dUC- and SEC-purified EVs revealed the presence of intact protein bands and well-defined migration patterns (Figure 1C), roughly indicating that both purification methods maintained the integrity of EV protein cargo. NTA of dUC-purified *S. sclarea* HR EVs showed a prominent peak at approximately 116 ± 15 nm (mode value) and a mean vesicle size distribution of 152 ± 12 nm (Figure 1D).

Approximately 90% of the detectable vesicles were within the 80–220 nm range. Furthermore, distribution analysis indicated that 67% of EVs had a hydrodynamic diameter <140 nm, whereas only 16% exceeded 200 nm, possibly due to EV aggregation. The EV concentration ranged from 1.5×10^{10} −7.8 x 10^{10} particles/mL. A comparable size distribution of EVs was obtained by SEC purification (Figure 1E), although the yield of EVs was much lower than that of dUC preparations (1.5×10^{9} – 8.3×10^{9} particles/mL).

Scanning (Figure 1F) and transmission electron micrographs (Figure 1G and H) of grouped and single *S. sclarea* EVs revealed round-shaped biogenic nanoparticles with the expected size. The size distribution, concentration, and morphology of *S. dominica* EVs are detailed in Figure S1 and closely alignwith the findings reported in our previous study.

Finally, to assess the absence of *A. rhizogenes* contamination in the EV samples, PCR amplification of fragments of *A. rhizogenes* genes such as *virD2* (317 bp), *rolB* (590 bp), and *rolC* (514 bp) was performed. As depicted in Figure 1I, EV samples derived from *S. sclarea* tested negative for *A. rhizogenes* genes, as also reported for *S. dominica* HR EVs[14] proving the absence of bacterial DNA in the HR EV preparations.

Protein Profiling of *Salvia sclarea* HR EVs

EVs contain unique sets of proteins that drive their biogenesis, release, and uptake by target cells, as well as other molecular signals that regulate various cellular functions in recipient cells. In our previous work, we reported a detailed proteomic characterization of *S. dominica* HR-derived EVs, showing that they carry typical EV-associated markers, such as cytoskeletal components, chaperone proteins, glyceraldehyde-3-phosphate dehydrogenases, and integral membrane proteins.[14]

In this study, we aimed to gain a thorough understanding of the protein composition of *Salvia sclarea* HRs and HR EVs, using a gel-based proteomic approach. Owing to the limited data available for *Salvia spp*. proteomes, protein identification was conducted using the broader Green Plant (Viridiplantae) protein database, which allowed the identification of 167 proteins in HR EVs and 1,206 proteins in HRs (Supplementary Information; Tables S2 and S3, respectively).

The HR EVs proteome showed proteins typically associated with plant EVs, such as ATP synthase subunits, nucleic acid binding proteins, ribosomal constituents, cytoskeleton elements (eg, actin), elongation factors, histones, molecular chaperones (such as HSP70), and many other membrane proteins, including vacuolar protein sorting-associated proteins (VPS26A and VPS20) and members of sugar transporters and ABC transporters (Table S2). Notably, we observed many peroxidases that might confer antioxidant activity to *Salvia* HR EVs.

To further characterize and investigate the potential biological relevance of HR EVs, we carried out a gene ontology (GO) analysis of Biological Processes (BP). Most proteins in the EVs proteome are involved in “response to stress” and “response to abiotic stimulus” categories (Figure 2A). These findings confirm that plant EVs serve as essential mediators in plant responses and signalling to various environmental factors, encompassing both biotic and abiotic constraints, and emphasize their key roles in plant defense mechanisms and interactions with the environment. To validate these findings, the proteome of HRs originating EVs was also studied. Despite the limitations of the protein database discussed above, more than 1,200 proteins were identified (Table S3), and their biological functions were in agreement with those expected for the proteome of a complex tissue (Figure 2B). Indeed, the HR proteome displays a broad range of metabolic activities, particularly the metabolism of small molecules and organic compounds.

As there are no reliable markers for HR-derived EVs, we performed a comparative analysis between the proteomes of *S. sclarea* and *S. dominica* HR EVs. This analysis revealed 15 proteins common to both species (Table S4), providing an initial set of candidate markers for *Salvia* EVs. We then checked whether these shared proteins were also found in the proteome of apoplastic EVs isolated from the model plant species *Arabidopsis thaliana*. This comparison revealed nine common proteins, as listed in Table S5, including a 14-3-3 like protein GF14, an ABC transporter G family member, actin, an ATP synthase A, a calcium-dependent protein kinase 20, glyceraldehyde-3-phosphate dehydrogenase 2, heat shock 70, NADP-dependent malic enzyme, and ribulose bisphosphate carboxylase/oxygenase activase. These common

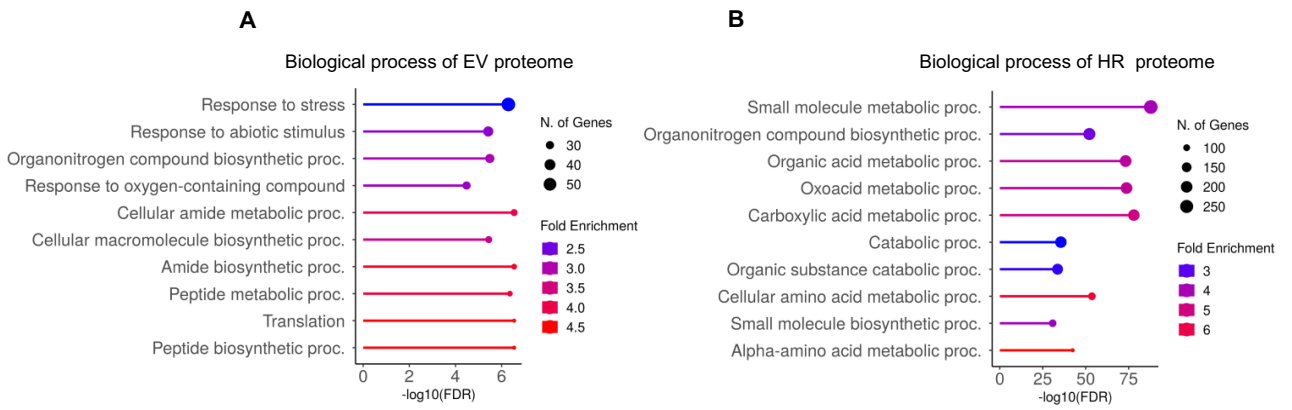

Figure 2 Results of gene ontology analysis of the HR EV and HR proteomes. Proteins identified in the HR EVs (**A**) and HR (**B**) proteomes were classified based on their biological functions. The number of proteins identified, fold enrichment, and the FDR are indicated.

proteins in phylogenetically distant species may represent the conserved components of the plant EV proteome. Finally, eight out of 15 common proteins detected in *Salvia sclarea* and *Salvia dominica* EVs have human homologues with a sequence identity >50% (Table S6). These homolog proteins are included in the EVs public database ExoCarta (http://www.exocarta.org).

S. sclarea and *S. dominica* HR EVs Transport Prevalently Terpenoids

Exploring the metabolomic profile of EVs holds the potential to elucidate their biological role in plant defense mechanisms and uncover potential human health benefits. To this aim, mass spectrometry-based metabolomic analyses were performed on both *S. sclarea* and *S. dominica* HR-EVs. The metabolic chromatograms of EVs derived from *Salvia spp*. exhibited a remarkable degree of similarity (Figure 3A).

These profiles were predominantly characterized by the presence of triterpenoid compounds, as shown in Figure 3B. More specifically, LC-MS analysis highlighted the presence of ursolic and oleanolic derivatives, particularly asiatic acid and its isomer ($C_{30}H_{48}O_5$).

These compounds have been previously reported to have pharmacological activities, including antibacterial, anti-dermatophytic, antioxidant, anti-inflammatory, antineoplastic, and anti-aggregant properties. Interestingly, asiatic, ursanic, and oleanolic acids have been documented to exert potent neuroprotective effects.

HR EVs Enter Dopaminergic Neurons and Alleviate 6-OHDA-Induced Neurotoxicity

To evaluate the potential neuroprotective properties of HR EVs, we tested them in SH-SY5Y cells, a human neuroblastoma derivative that offers a practical and sustainable alternative to primary human dopaminergic neurons. Widely utilized in studying neurological disorders, SH-SY5Y cells combined with neurotoxin treatments serve as an in vitro model for investigating the cellular and molecular basis of neurological disorders and for preliminary drug screening in Parkinson's disease (PD).

To test the safety of EVs, SH-SY5Y cells were treated with increasing concentrations of HR EVs (10^4–10^8 particles/mL) for 24 h, and cell viability was assessed using an MTT assay. As shown in Figure S2, application of HR-derived EVs had no detrimental effects on SH-SY5Y cells.

Subsequently, we examined the cellular uptake of HR-derived extracellular vesicles by exposing SH-SY5Y cells to BODIPY-labelled EVs (1.2 x 10^8 particles/mL) for 24 h. As expected, control cells did not show fluorescence in the green channel (Figure 4A–D), whereas confocal microscopy revealed extensive and diffuse EV uptake in SH-SY5Y (Figure 4E–H). Internalized HR EVs appeared to be uniformly distributed in the cytoplasm and perinuclear regions of the recipient cells. As an additional control, EV-depleted medium containing excess free dye was added to the cells. This resulted in a distinct staining pattern characterized by large fluorescent spots (Figure S3), likely due to the aggregation or cellular compartmentalization of residual BODIPY.

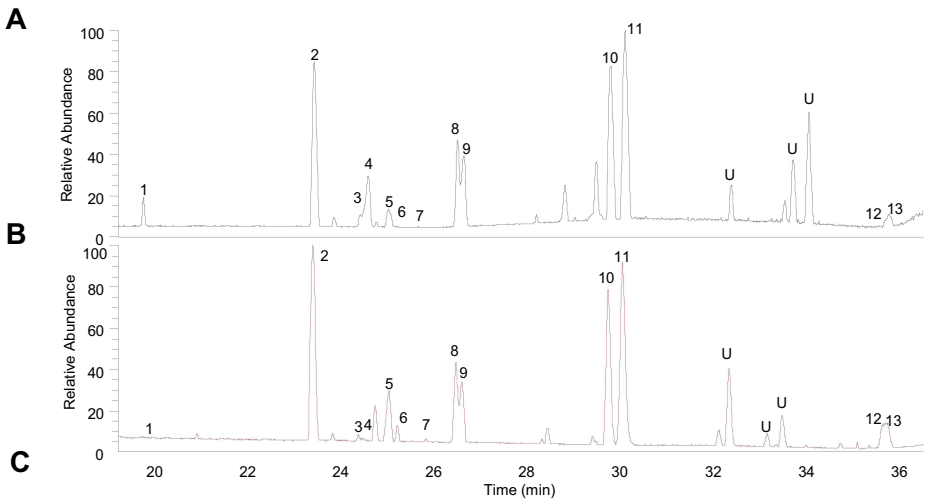

N°	Rt (min)	Molecular formula	[M+H]⁻ /[M+H]⁺	Compound	MSI status#
1	19.71	$C_{30}H_{48}O_6$	503.3380	Triterpene	3
2	23.36	$C_{30}H_{48}O_5$	487.2433	Asiatic Acid	1
3	24.51	$C_{30}H_{48}O_5$	487.2433	Triterpene	3
4	24.85	$C_{30}H_{48}O_5$	487.2433	Triterpene	3
5	25.00	$C_{30}H_{48}O_5$	487.2433	Ursan-12-en-28-oic acid, 2α,3α,23-Trihydroxy	1
6	25.18	$C_{30}H_{48}O_6$	503.3380	Triterpene	3
7	25.79	$C_{30}H_{48}O_6$	503.3380	Triterpene	3
8	26.43	$C_{30}H_{48}O_5$	487.2433	Arjunolic acid	1
9	26.57	$C_{30}H_{48}O_5$	487.2433	Ursan-12-en-28-oic acid, 3β,20,23-Trihydroxy	1
10	29.7	$C_{30}H_{48}O_4$	471.3434	Ursan-12-en-28-oic acid, 2,3-dihydroxy	1
11	30.02	$C_{30}H_{48}O_4$	471.3434	aslinic acid	3/2
12	35.58	$C_{30}H_{48}O_3$	455.3527	Oleanolic Acid	1
13	35.68	$C_{30}H_{48}O_3$	455.3527	Ursolic Acid	1
U	32.00-34.00			Unidentified compounds	

Figure 3 Metabolomic analysis of EVs of *S. sclarea* and *S. dominica* hairy roots. (**A** and **B**) Representative chromatograms showing the metabolomic profiles of *S. sclarea* and *S. dominica* HR EVs, respectively. (**C**) List of specialized metabolites detected in HR EVs of *S. sclarea* and *S. dominica* by UHPLC-HR-ESI-Orbitrap/MS. MSI status# in c: Metabolomics Standards Initiative.

Then, we co-administered to SH-SY5Y cells EVs derived from *S. sclarea* along with various neurotoxic agents, such as 1 μM mitoxantrone (Figure 4I), 40 μM Aβ (1–42) (Figure 4J), 400 μM H_2O_2 (Figure 4K), and 100 μM 6-OHDA (Figure 4L), and tested the cell viability using the MTT assay. Overall, HR EVs significantly alleviated neurotoxicity in all the tested treatments. Impressively, HR EVs almost completely suppressed the toxicity of 6-OHDA. More specifically, we found that the incubation of SH-SY5Y cells with only 6-OHDA reduced cell viability to 10.02 ± 0.25% and 13.12 ± 1.52% (Figure 4F) compared to control cells, whereas co-administration of HR EVs completely preserved cell viability up to 97.15 ± 2.41% ($p< 0.001$ vs 6-OHDA; (Figure 4F) and 95.52 ± 1.97% ($p < 0.001$ vs 6-OHDA; Figure 4D), respectively. HR non-conditioned medium and EV-depleted media of *S. sclarea* and *S. dominica* were used as experimental controls, which showed no significant reduction in 6-OHDA toxicity (Figure S4). Worth noting, protective effects were not observed when HR EVs were administered 24 h before or 24 after 6-OHDA treatment, as shown in Figure S5. Taken together, these data suggest that neuroprotective effects are specifically associated with the presence of EVs, which can directly neutralize the detrimental effects of 6-OHDA.

EVs bioactivity was also evaluated by flow cytometry to corroborate their protective effects against 6-OHDA-induced apoptosis. The incubation of SH-SY5Y cells with 6-OHDA for 24 h increased the percentage of hypodiploid nuclei. On the other hand, co-administration of HR EVs reduced the number of cells undergoing apoptosis from 38.44 ± 3.21% (6-OHDA alone) to 7.12 ± 4.10% (*S. sclarea* EVs/6-OHDA co-administration) ($p < 0.001$ vs 6-OHDA) (Figure 4M) and

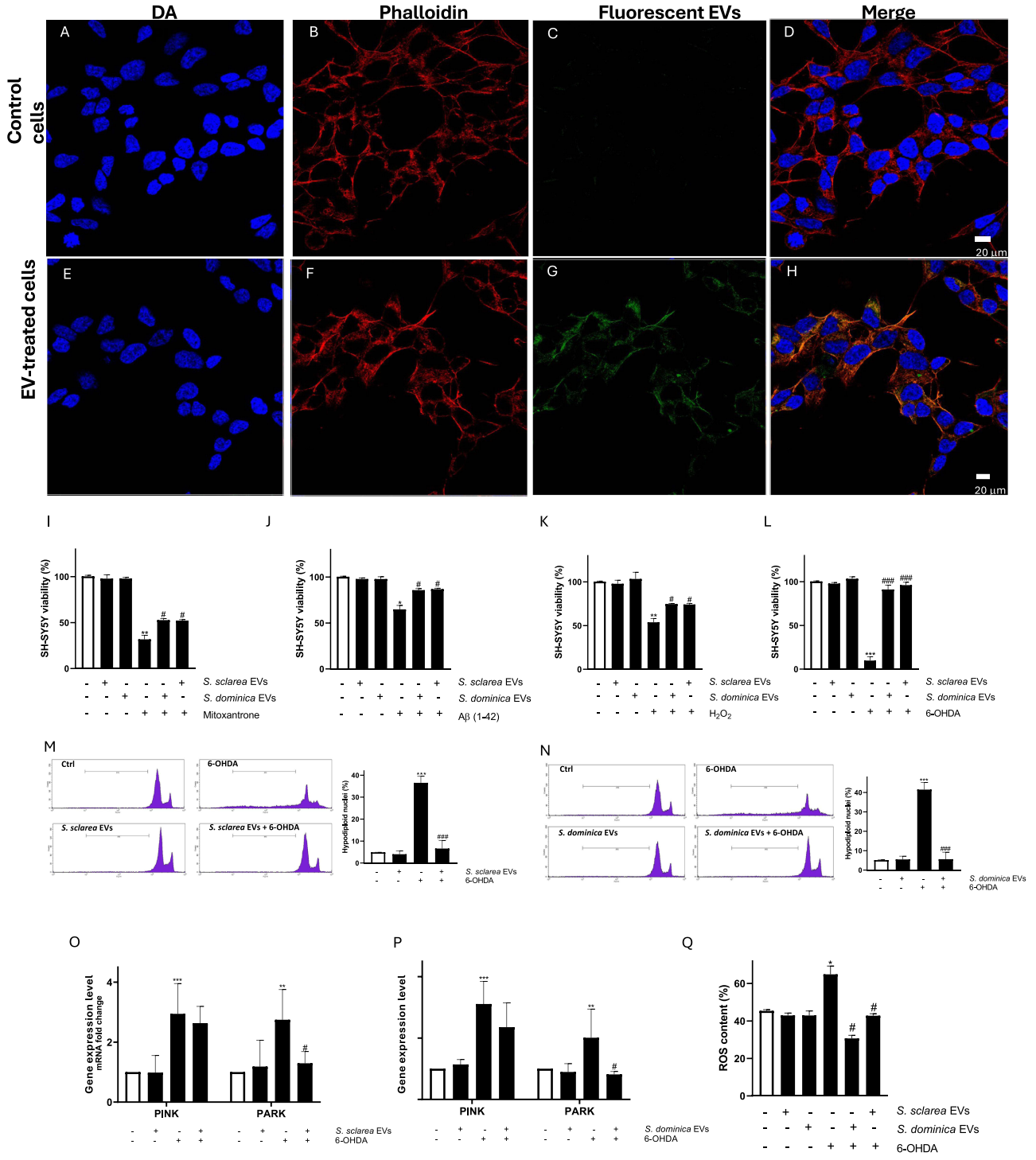

Figure 4 Evaluating neuroprotective effects of *S. sclarea* and *S. dominica* EVs against 6-OHDA-induced SH-SY5Y. (**A**–**D**) Representative confocal microscopy imaging of SH-SY5Y control cells. (**E**–**H**) Representative confocal microscopy analysis of SH-SY5Y cells treated with BODIPY-stained EVs (1.2×10^8 particles/mL) of *S. sclarea* HRs for 24 h. Cells have been stained with phalloidin-TRITC (actin, red). Nuclei were stained with DAPI. Magnification 63×/1.4 numerical aperture. Scale bar = 20 mm in (**D**) and (**H**). (**I**–**M**) Neuroprotective effects of *S. sclarea* and *S. dominica* upon administration of 1 µM mitoxantrone (**I**), 40 µM Aβ (1–42) (**J**), 400 µM H_2O_2 (**K**) and 100 µM 6-OHDA (**L**). The viability variations were determined by calculating the percentage of viable cells in treated cultures in comparison to untreated ones. (**M** and **N**) Evaluation of apoptosis in SH-SY5Y cells by propidium iodide assay through flow cytometry upon co-administration of *S. sclarea* and *S. dominica* HR EVs, respectively. Data are expressed as percentage of hypodiploid nuclei. (**O** and **P**) *PINK1* and *PARK2* mRNA levels by qRT-PCR in SH-SY5Y cells upon co-administration of *S. sclarea* and *S. dominica* EVs, respectively. *GAPDH* was used as housekeeping control. The $2^{-\Delta\Delta CT}$ method was employed to calculate the expression fold changes relative to untreated cells. (**Q**) Spectrophotometric fluorescence intensity measurement showing the protective role of HR EVs in SH-SY5Y treated with 100 µM 6-OHDA. All results are showed as mean ± standard deviation from three independent experiments conducted with dUC and SEC-purified EVs. *, **, ***Denote respectively $p < 0.05$, $p < 0.01$ and $p < 0.001$ vs Ctrl; # and ###Denote respectively $p < 0.05$ and $p < 0.001$ vs 6-OHDA.

from 41.12 ± 2.89% (6-OHDA alone) to 4.88 ± 3.11% (*S. dominica* EVs/6-OHDA co-administration) ($p < 0.001$ vs 6-OHDA; Figure 4N). Thus, when treated with 6-OHDA and HR EVs, the observed apoptosis levels in cells were not significantly different from those in control cells.

We then evaluated the expression of *(PTEN)-induced putative kinase 1* (*PINK1*) and *Parkinson's disease 2* (*PARK2/parkin*) genes, which are typically involved in the clearance of damaged mitochondria via mitophagy.[26] As expected, the exposure of SH-SY5Y cells to 6-OHDA for 24 h significantly enhanced the levels of *PINK1* and *PARK2* genes ($p < 0.01$ vs Ctrl) (Figure 4O and P). The levels of *PINK1* and *PARK2* transcripts were not significantly altered by EV treatment alone (1.3 ± 0.15-fold down; $p < 0.01$ vs 6-OHDA for *PINK1*, 1.3 ± 0.1-fold down, $p < 0.01$ vs 6-OHDA for *PARK2*). In contrast, co-administration of EVs derived from both *S. sclarea* and *S. dominica* HRs prevents the overexpression of *PARK2*, implying a potential mitigating role against 6-OHDA-associated mitochondrial damage in an in vitro model of Parkinson's disease.

Finally, due to the well-known detrimental effects of ROS in neuronal cells exposed to 6-OHDA, we assessed the ability of HR EVs to mitigate the production of these oxidative molecules. The data shown in Figure 4Q demonstrate that the co-administration of HR EVs effectively reduced 6-OHDA-induced ROS levels back to endogenous cell levels ($p < 0.05$, 6-OHDA). Collectively, these data demonstrated that HR EVs inhibited the development of Parkinson's disease cellular changes in 6-OHDA-treated SH-SY5Y cells.

HR EVs Prevent Metabolome Changes Induced by 6-OHDA

Given the intricate interplay between metabolites, redox homeostasis, and bioenergetics in Parkinson's disease, metabolomics may be instrumental in understanding the distinctive cellular features of this disease and may contribute to the development of new therapeutic interventions. Therefore, we profiled metabolomic changes in our experimental system. The metabolites were extracted from the cell pellets and analyzed in both polarities using UHPLC-ESI-MS/MS. Significant metabolomic variations were observed specifically in the metabolome acquired in the positive ionization mode. Principal component analyses (PCA) displayed in Figure 5A and B showed significant metabolomic dysregulation in SH-SY5Y cells treated with 6-OHDA, which was not detected upon EV co-administration. Notably, HR EVs alone did not significantly modify cell metabolic homeostasis compared to control cells.

Among the metabolic pathways mainly affected by 6-OHDA, we observed enrichment in glutathione metabolism, showing a disruption in the cellular redox balance, as expected. Notably, within the key metabolites of glutathione metabolism, our analysis revealed the abundance of L-cystathionine, gamma-glutamylglutamic acid, S-(hydroxymethyl) glutathione, and both oxidized and reduced forms of glutathione (Tables S7 and S8).

Interestingly, we also observed many other metabolites involved in the cell stress response and detoxification, including N-acetyl-L-histidine, L-methionine, L-glutamine, imidazoleacetic acid, and hypotaurine. Furthermore, we observed the impairments in other interconnected pathways, such as "Nicotinate and nicotinamide metabolism", "Pentose and glucuronate interconversions", and numerous pathways involved in amino acid biosynthesis and metabolism impacting fundamental cell processes including cellular energy, antioxidant defenses, protein homeostasis and mitochondrial function. Lastly, increased levels of dimethylethanolamine and sn-glycero-3-phosphoethanolamine were found, indicating alterations in the membrane composition and integrity.

Collectively, these findings demonstrated the efficacy of HR EVs from *S. sclarea* and *S. dominica* in mitigating the detrimental effects of 6-OHDA by efficiently reducing oxidative stress and significantly preventing metabolic shifts induced by 6-OHDA.

HR EVs Inhibit 6-OHDA Autoxidation and p-Quinone Formation

The next question we addressed aimed to understand the potential mechanism by which EVs derived from Salvia HR prevent oxidative stress. One of the well-characterized oxidation products of 6-OHDA is *p*-quinone, a primary mediator of ROS production that contributes to nerve cell damage and neurotoxicity.[27,28] Therefore, we monitored its formation in a cell-free system over time, both with and without HR EVs. The antioxidant NAC (N-acetyl cysteine) was used as a positive control. Notably, EVs exhibited a potent antioxidant effect in vitro, prompting an extension of the time course beyond the durations described in previous studies that used NAC as a reference antioxidant because its effect was only

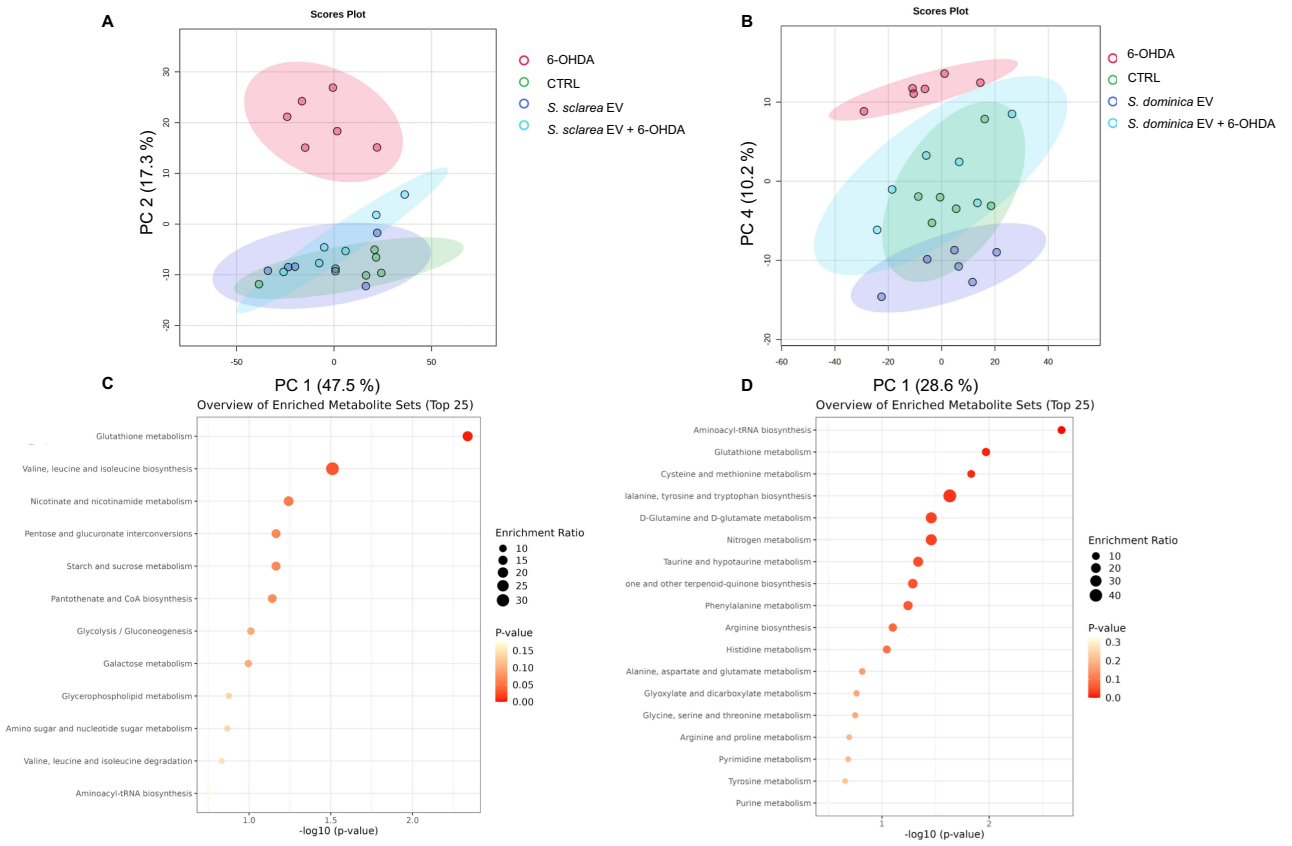

Figure 5 Untargeted metabolomics profiling to study the neuroprotective effects of HR EVs. (**A** and **B**) Principal component analysis of metabolomic data demonstrating good separation of 6-OHDA-treated groups with respect to treatments with *S. sclarea* and *S. dominica* HR EVs, respectively. (**C** and **D**) Enrichment analysis to functionally classify the differentially expressed metabolites in 6-OHDA compared to treatments with *S. sclarea* and *S. dominica* HR EVs, respectively. The enrichment ratio, beside the plots, is indicated by the proportional diameter size of the black circles.

observed within the first 10 min of 6-OHDA autoxidation. In contrast, both *S. sclarea* (Figure 6A) and *S. dominica* EVs (Figure 6B) prevented autoxidation, with a unique feature that their defensive effects remained significant at 8 h. To eliminate the potential interference of fetal bovine serum components (EVs, lipids, lipoproteins, etc).,[29] we conducted this assay in a serum-deprived medium. These data indicate that *S. sclarea* and *S. dominica* EVs offer neuroprotection, likely by acting on 6-OHDA autoxidation in a more effective way than NAC, which is one of the most potent inhibitors of *p*-quinone formation.[24,30]

To further test this hypothesis, we evaluated in vitro the conversion of *p*-quinone into non-toxic melanin. Based on EVs' strong ability to neutralize *p*-quinone, we expected minimal melanin formation because the levels of *p*-quinone, the precursor of melanin, would already be reduced. As shown in Figure 6C and D, the presence of ferrous ions indeed increased melanin formation, consistent with previous research.[25] However, the presence of HR EVs significantly reduced melanin formation, even below the levels seen with 6-OHDA alone. This confirmed the selective counteraction mechanism of *S. sclarea* and *S. dominica* EVs in *p*-quinone formation.

Discussion

Plant EVs represent a safe, viable and effective alternative to mammalian EVs in nanomedicine.[13] Large-scale production of plant EVs can benefit from the use of cell cultures and hairy roots, which are widely used as biofactories to produce commercially interesting bioactive ingredients with pharmaceutical, nutraceutical and cosmetic value. These plant biotechnological platforms offer a plethora of advantages such as cost-effectiveness, scalability, contaminant-free conditions, and bio-sustainable processes for the production of desired compounds applicable at an industrial scale.[17]

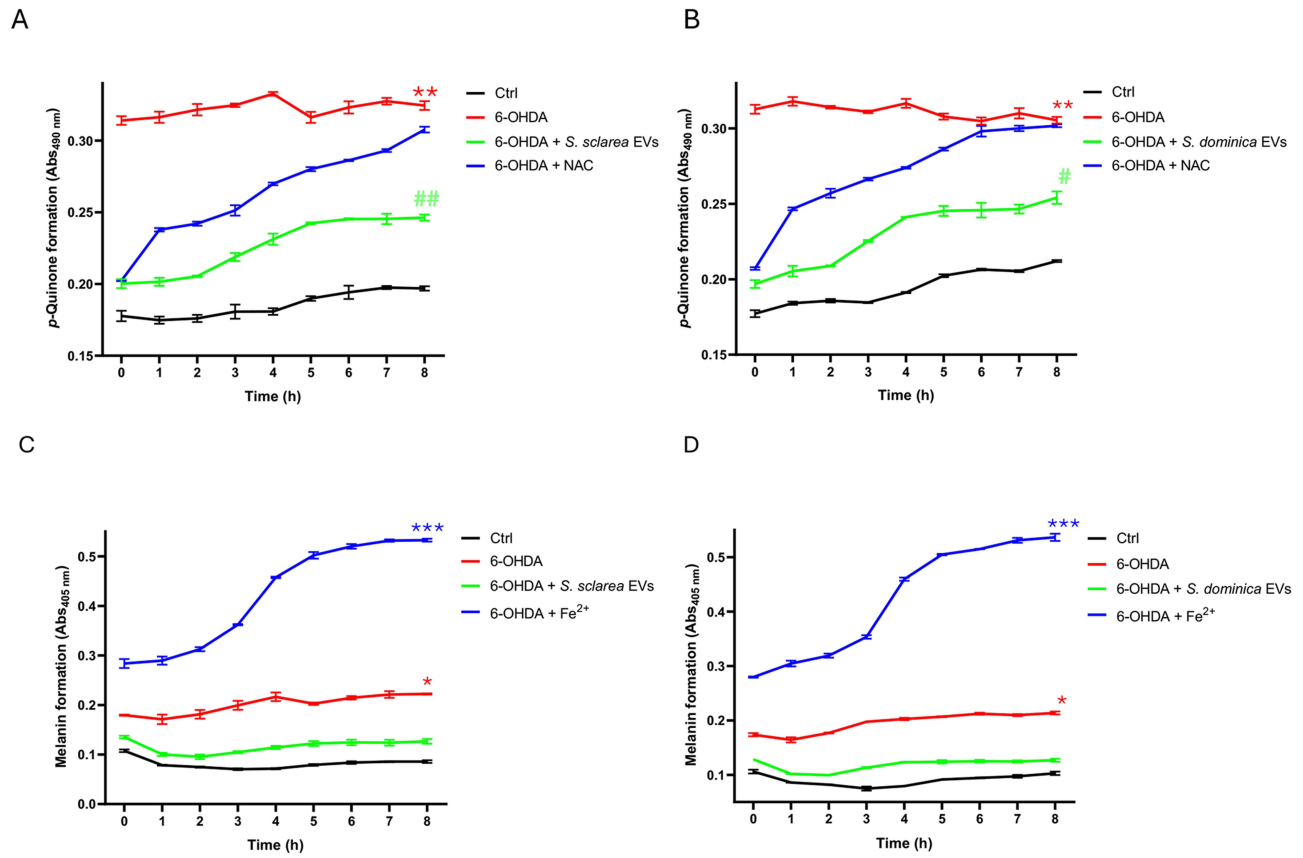

Figure 6 Biochemical effects of *S. sclarea* and *S. dominica* HR EVs against 6-OHDA autoxidation. The formation of *p*-quinone was monitored at 490 nm in DMEM without serum with *S. sclarea* (**A**) or *S. dominica* (**B**) HR EVs using NAC (1 mM) as a positive control. The melanin formation assay was performed in a cell-free system, and the product was spectrophotometrically measured every 1 h. Melanin formation was monitored at 405 nm in DMEM without serum with *S. sclarea* (**C**) or *S. dominica* (d) HR EVs, using Fe^{2+} (300 µM) as a positive control. The results are presented as mean ± standard deviation (SD) from two independent experiments. *, **, *** denote respectively $p < 0.05$, $p < 0.01$ and $p < 0.001$ vs Ctrl; # and ## denote respectively $p < 0.05$, $p < 0.01$ and $p < 0.001$ vs 6-OHDA.

Here, we report the use of HRs from *Salvia spp*. as an alternative source of EVs and their potential applications in neuroprotection. The choice to study EVs released from *Salvia* species was based on their long-standing applications in traditional medicine, owing to the well-proven bioactivity of their secondary metabolites against different human diseases. *S. sclarea* is regularly consumed as a food product, and its essential oils are generally recognized as safe by the Food and Drug Administration.[31] *S. dominica* is currently considered an important wild genetic resource within *Salvia* genus as a source of health-promoting compounds.[32]

We set up a reproducible purification of EVs released from HRs either from *S. dominica* or *S. sclarea*, having size and morphology comparable to those of EVs purified from different plant species.[33–35] We compared well-established EV purification techniques and found that overall dUC isolation method ensures higher EV yield with respect to SEC in our experimental system. However, we expect that methods suitable for large-scale research applications (eg, tangential flow filtration) and novel strategies (eg, HR elicitation by biological, chemical, and physical stimuli) may further maximize the EV yield, as reported in mammalian systems.[36]

Proteome comparative analysis clearly showed that *S. sclarea* EVs carry a specific protein biocargo that differs from the protein composition of the HRs from which they are released. The enrichment analysis of GO terms and protein domains indicated that many proteins carried by EVs participate in diverse plant stress responses, defense mechanisms, and intercellular communication, as extensively reported in recent years.[3,18,35,37,38]

We also identified ATP synthase subunits, ribosomal constituents, cytoskeletal elements (eg, actin), elongation factors, molecular chaperones (such as HSP70), vacuolar protein sorting-associated proteins (VPS26A and VPS20),

and members of sugar transporters and ABC transporters (Table S3), which have been recurrently found in plant EV proteomes[39] and in the Exocarta and Vesiclepedia databases.

By comparing the proteomes of *S. sclarea* and *S. dominica* HR EVs, we identified a shared set of proteins. In addition to frequently associated EV proteins, such as Actin, Elongation factor 1-alpha, ATPase subunit alpha, HSP 70, and glyceraldehyde-3-phosphate dehydrogenase 2, our results revealed novel potential specific markers of *Salvia* EVs, including TIFY 10A, alpha-mannosidase, and berberine bridge enzyme-like. These findings expand our understanding of plant EV biomarkers and provide new anchor proteins for EV bioengineering.

In the broader context of the *Salvia* genus, terpenoids and polyphenols have been reported as the main specialized metabolites. Previous studies have identified phenolic acids, flavonoids, and terpenoids in aerial parts, whereas oxygenated abietane-type diterpenes with a common ortho- or para-quinone chromophore are more prevalent in the roots.[40] HRs of *S. sclarea* are recognized for the production of various diterpenoids and triterpenoids, including ferruginol, salvipisone, aethiopinone, 1-oxoaethiopinone, oleanolic acid, ursolic acid, 2α,3α-dihydroxy-urs-12-en-28-oic acid, and 2α,3α,24-trihydroxy-urs-12-en-28-oic acid.[41,42] The current understanding of specialized metabolites transported by plant EVs is still limited, and the factors influencing this process remain underexplored. Our results provide evidence for a straightforward connection between EV metabolomic profiles and tissue of origin and subcellular compartments. Specifically, the metabolomic profiles of *S. sclarea* and *S. dominica* HR EVs revealed high similarity in their metabolomic profiles, with triterpenoids being the predominant constituents of the EVs' metabolomic cargo. The data indicate a shared mechanism in different species for incorporating molecules into EVs, likely influenced by the high concentration and hydrophobic or amphiphilic nature of these molecules in *Salvia* HRs. This assumption aligns with previous observations reporting similar enrichment of lipophilic molecules in EVs derived from various plant sources, including apoplastic fluid, cell culture media, and homogenized plant tissues.[34] However, it is important to consider that alternative loading mechanisms might play a role in concentrating specialized metabolites within plant EVs. Notably, ATP-Binding Cassette transporters (ABC transporters), identified in the HR EVs proteome and also observed in other plant EVs[18,35] could potentially contribute to facilitating the targeted loading of metabolites in EVs. Future studies employing genetic mutants of these transporters are required to validate this hypothesis.

The prevalence of triterpenoids in the metabolomic cargo of HR EVs also suggests a functional implication in plant defence mechanisms against harmful pests and pathogenic microbes, which might also have potential benefits for human health. Indeed, given their intricate chemical structures, triterpenoids exhibit interesting biological activities including antitumor, antiviral, antibacterial, and antioxidant properties.[43–45]

In this study, we focused on the possible beneficial effects of plant EVs on cellular and metabolic changes associated with PD, one of the most common neurodegenerative disorders, characterized by the progressive loss of dopaminergic neurons in the substantia nigra, leading to motor and non-motor dysfunction. It has been proposed that the PD onset might be triggered by oxidative damage, neuroinflammation, exposure to environmental toxins, genetic predisposition, and accelerated aging and other factors.[46]

Nanosized EVs have emerged as innovative carriers of therapeutic drugs and bioactive proteins for the treatment of PD. However, the concrete risk that mammalian-derived EVs carry pathological miRNAs and/or proteins[47,48] involved in the spread of neurological diseases has prompted research toward the identification of alternative EV sources.

In this study, we assessed the protective activity of HR EVs in neuroblastoma SH-SY5Y cells, an in vitro model widely used in PD research. To induce the manifestation of a PD-like phenotype in these cells, we administered 6-OHDA, which triggers neurotoxicity by preferentially accumulating within catecholaminergic neurons via dopamine transporters. This accumulation disturbs metabolic homeostasis, induces mitochondrial dysfunctions, and ultimately leads to significant neuronal damage.[49] Although this in vitro model does not completely mirror the complexities of PD, it is a fundamental tool to study the cell and molecular basis of PD pathogenesis and to test the efficacy of novel therapeutic interventions.[50]

We report the widespread uptake and safety profile of HR EVs in SH-SY5Y cells. When co-administered with 6-OHDA, HR EVs demonstrated significant neuroprotective activity, effectively inhibiting cellular damage and the metabolic alterations associated with PD. HR EVs preserved cell viability and dramatically reduced 6-OHDA-mediated apoptosis in SH-SY5Y cells. The involvement of mitochondrial damage in PD pathogenesis is well-established[51] and our findings revealed that treatment with HR EVs prevents the overexpression of *PARK2* gene, which encodes a protein

associated with mitochondrial dysfunction,[52] leading to neuronal death in PD, suggesting a potential mitigating role against 6-OHDA-associated mitochondrial damages.

Oxidative stress and metabolic dysregulation areinherent features of PD. Our data confirmed this correlation, since 6-OHDA treatment elevated ROS levels and profoundly altered cellular metabolism, impacting essential biological pathways, including amino acid biosynthesis, cellular energy, antioxidant defenses, protein homeostasis, and mitochondrial function. Remarkably, co-administration of HR EVs significantly contributed to the preservation of metabolic homeostasis, which was severely affected by 6-OHDA treatment.

As the HR EVs of these two *Salvia* species exhibit shared metabolic cargo, the mitigation of oxidative stress could be attributed to the presence of therapeutic triterpenoids in the EV biocargo. Notably, among the transported triterpenoids in HR EVs, asiatic acid,[53,54] ursolic acid,[55,56] maslinic acid[57] and oleanolic acid,[58–60] have been well-documented for their robust neuroprotective activity in vitro and in vivo. Additionally, the antioxidant activity of enzymes delivered by HR EVs (eg, peroxidases) may exert a synergistic effect in preventing neuronal oxidative damage in response to 6-OHDA.

6-hydroxydopamine is a relatively unstable molecule that is prone to both enzymatic and nonenzymatic oxidation processes. For example, monoamine oxidase oxidizes 6-OHDA to produce H_2O_2, which initiates the production of oxygen radicals. Additionally, 6-OHDA's auto-oxidation generates H_2O_2, ROS, and catecholamine quinones, resulting in rapid depletion of endogenous antioxidant enzymes. It has been reported that in cellular models that express diminished levels of dopamine transporters (DAT), such as undifferentiated SH-SY5Y cells, in combination with elevated concentrations of 6-OHDA (ranging from 100 to 150 μM), the auto-oxidation of the toxin predominantly takes place in the extracellular medium.[61] By using a cell-free system, we effectively showed that HR EVs inhibit the auto-oxidation of 6-OHDA and the subsequent formation of *p*-quinone. This led to the conclusion that the antioxidant bioactivity of HR EVs is likely initiated at the extracellular level. This finding is of significant pharmacological interest, implying that HR EVs have an inherent capacity to neutralize neurotoxic metabolites in the circulation.

Furthermore, our data revealed that HR EVs penetrated cells, delivering a rich array of antioxidants. This intracellular cargo might play a crucial role in combating oxidative stress in cells. It helps to preserve the function of various organelles and supports the maintenance of metabolic equilibrium in a Parkinson's disease model. This dual action, both extracellular and intracellular, of HR EVs emphasizes their potential as a novel therapeutic tool for managing neurodegenerative disorders, such as Parkinson's disease.

Conclusion

The use of HRs as an alternative source of plant EVs offers significant advantages in terms of industrial production and therapeutic potential. We provide straightforward evidence that HR EVs from *Salvia spp*. have strong and multifaceted neuroprotective effects, including the inhibition of toxicity, modulation of mitochondrial function, metabolic regulation, and neutralization of neurotoxic molecules. Building on these findings, HR EVs from *S. sclarea* and *S. dominica* deserve clinical investigation as promising candidates for developing new pharmaceutical and nutraceutical strategies to prevent and mitigate the effects of neurotoxins. However, it is crucial to first conduct rigorous preclinical studies to thoroughly evaluate their safety, efficacy, and mechanisms of action before advancing to human trials.

Abbreviations

EVs, extracellular vesicles; HRs, hairy roots; dUC, Differential Ultracentrifugation; SEC, Size Exclusion Chromatography; NTA, Nanoparticle tracking analysis; 6-OHDA, 6-hydroxydopamine; PDVs, Plant-derived nano-and microvesicles; PD, Parkinson's Disease; SEM, Scanning electron microscopy; TEM, Transmission electron microscopy; UHPLC, ultra-high-performance liquid chromatography; LC-MS, liquid chromatography-mass spectrometry; MS, mass spectrometry; FBS, fetal bovine serum; DAPI, 4',6-diamidino-2-phenylindole; MTT, 3-[4,5-dimethylthiazol-2,5-diphenyl-2H-tetrazolium bromide; PCR, Polymerase Chain Reaction; qRT-PCR, Quantitative Reverse Transcription Polymerase Chain Reaction; ROS, Reactive Oxygen Species; NAC, N-acetyl cysteine; HSP, Heat shock protein; ABC transporter, ATP-Binding Cassette transporter.

Data Sharing Statement

The detailed experimental methods and additional figures are provided in the Supplementary Materials. Mass spectrometry proteomics of *S. sclarea* HRs and HR EVs were performed using ProteomeXchange with the identifier PXD048610. All other data from this study are available from the corresponding authors upon reasonable request.

Consent for Publication

All the authors agree to the publication of the article.

Acknowledgments

We would like to express our sincere gratitude to Prof. Ammar Bader (Faculty of Pharmacy Umm Al-Qura University Makkah, Saudi Arabia) for his invaluable assistance in identifying the *S. dominica* species and generously providing us with the seeds.

Author Contributions

All authors made a significant contribution to the work reported, whether that is in the conception, study design, execution, acquisition of data, analysis and interpretation, or in all these areas; took part in drafting, revising or critically reviewing the article; gave final approval of the version to be published; have agreed on the journal to which the article has been submitted; and agree to be accountable for all aspects of the work.

Funding

This study was supported by the following projects: SecrEVome project (Grant number:202224M943) funded under the PRIN 2022 program of the Italian Ministry of University and Research, funded by the European Union's NextGenerationEU; "National Biodiversity Future Center - NBFC" funded under the National Recovery and Resilience Plan (NRRP), Mission 4 Component 2 Investment 1.4 - Call for tender No. 3138 of December 16, 2021, rectified by Decree n.3175 of December 18, 2021, of Italian Ministry of University and Research funded by the European Union – NextGenerationEU, Project code CN_00000033, Concession Decree No. 1034 of June 17, 2022, adopted by the Italian Ministry of University and Research, CUP: D43C22001260001.

Disclosure

The authors declare that they have no conflicts of interest in this work.

References

1. Théry C, Witwer KW, Aikawa E, et al. Minimal information for studies of extracellular vesicles 2018 (MISEV2018): A position statement of the international society for extracellular vesicles and update of the MISEV2014 guidelines. *J Extracell Vesicles*. 2018;7(1):1535750. doi:10.1080/20013078.2018.1535750
2. Welsh JA, Goberdhan DCI, O'Driscoll L, et al. Minimal information for studies of extracellular vesicles (MISEV2023): From basic to advanced approaches. *J Extracell Vesicles*. 2024;13(2):e12404. doi:10.1002/jev2.12404
3. Chen Y, Xu Y, Zhong H, et al. Extracellular vesicles in inter-kingdom communication in gastrointestinal cancer. *Am J Cancer Res*. 2021;11(4):1087–1103.
4. Raposo G, Stahl PD. Extracellular vesicles: A new communication paradigm? *Nat Rev Mol Cell Biol*. 2019;20(9):509–510. doi:10.1038/s41580-019-0158-7
5. Cai Q, Qiao L, Wang M, et al. Plants send small RNAs in extracellular vesicles to fungal pathogen to silence virulence genes. *Science*. 2018;360(6393):1126–1129. doi:10.1126/science.aar4142
6. Herrmann IK, Wood MJA, Fuhrmann G. Extracellular vesicles as a next-generation drug delivery platform. *Nat Nanotechnol*. 2021;16(7):748–759. doi:10.1038/s41565-021-00931-2
7. Alvarez-Erviti L, Seow Y, Yin H, Betts C, Lakhal S, Wood MJA. Delivery of siRNA to the mouse brain by systemic injection of targeted exosomes. *Nat Biotechnol*. 2011;29(4):341–345. doi:10.1038/nbt.1807
8. Sardar Sinha M, Ansell-Schultz A, Civitelli L, et al. Alzheimer's disease pathology propagation by exosomes containing toxic amyloid-beta oligomers. *Acta Neuropathol*. 2018;136(1):41–56. doi:10.1007/s00401-018-1868-1
9. Yin H, Hu J, Ye Z, Chen S, Chen Y. Serum long non-coding RNA NNT-AS1 protected by exosome is a potential biomarker and functions as an oncogene via the miR-496/RAP2C axis in colorectal cancer. *Mol Med Rep*. 2021;24(2):585. doi:10.3892/mmr.2021.12224
10. Janouskova O, Herma R, Semeradtova A, et al. Conventional and nonconventional sources of exosomes–isolation methods and influence on their downstream biomedical application. *Front Mol Biosci*. 2022;9:846650. doi:10.3389/fmolb.2022.846650

11. Stanly C, Alfieri M, Ambrosone A, Leone A, Fiume I, Pocsfalvi G. Grapefruit-derived micro and nanovesicles show distinct metabolome profiles and anticancer activities in the A375 human melanoma cell line. *Cells*. 2020;9(12):2722. doi:10.3390/cells9122722
12. Alfieri M, Leone A, Ambrosone A. Plant-derived nano and microvesicles for human health and therapeutic potential in nanomedicine. *Pharmaceutics*. 2021;13(4):498. doi:10.3390/pharmaceutics13040498
13. Ambrosone A, Barbulova A, Cappetta E, et al. Plant extracellular vesicles: Current landscape and future directions. *Plants*. 2023;12(24):4141. doi:10.3390/plants12244141
14. Boccia E, Alfieri M, Belvedere R, et al. Plant hairy roots for the production of extracellular vesicles with antitumor bioactivity. *Commun Biol*. 2022;5(1):848. doi:10.1038/s42003-022-03781-3
15. Giri A, Narasu ML. Transgenic hairy roots. Recent trends and applications. *Biotechnol Adv*. 2000;18(1):1–22. doi:10.1016/s0734-9750(99)00016-6
16. Sonkar N, Shukla PK, Misra P. Plant hairy roots as biofactory for the production of industrial metabolites. In: *Plants as Bioreactors for Industrial Molecules*. John Wiley & Sons, Ltd; 2023:273–297. doi:10.1002/9781119875116.ch11
17. Srivastava S, Srivastava AK. Hairy root culture for mass-production of high-value secondary metabolites. *Crit Rev Biotechnol*. 2007;27(1):29–43. doi:10.1080/07388550601173918
18. Rutter BD, Innes RW. Extracellular vesicles isolated from the leaf apoplast carry stress-response proteins. *Plant Physiol*. 2017;173(1):728–741. doi:10.1104/pp.16.01253
19. Sumner LW, Amberg A, Barrett D, et al. Proposed minimum reporting standards for chemical analysis chemical analysis working group (CAWG) metabolomics standards initiative (MSI). *Metabolomics off J Metabolomic Soc*. 2007;3(3):211–221. doi:10.1007/s11306-007-0082-2
20. Di Sarno V, Giovannelli P, Medina-Peris A, et al. New TRPM8 blockers exert anticancer activity over castration-resistant prostate cancer models. *Eur J Med Chem*. 2022;238:114435. doi:10.1016/j.ejmech.2022.114435
21. Sellitto A, Geles K, D'Agostino Y, et al. Molecular and functional characterization of the somatic PIWIL1/piRNA pathway in colorectal cancer cells. *Cells*. 2019;8(11):1390. doi:10.3390/cells8111390
22. Aquino G, Basilicata MG, Crescenzi C, et al. Optimization of microwave-assisted extraction of antioxidant compounds from spring onion leaves using box–behnken design. *Sci Rep*. 2023;13(1):14923. doi:10.1038/s41598-023-42303-x
23. Pfaffl MW. A new mathematical model for relative quantification in real-time RT–PCR. *Nucleic Acids Res*. 2001;29(9):45e–45. doi:10.1093/nar/29.9.e45
24. Lin YP, Chen TY, Tseng HW, Lee MH, Chen ST. Chemical and biological evaluation of nephrocizin in protecting nerve growth factor-differentiated PC12 cells by 6-hydroxydopamine-induced neurotoxicity. *Phytochemistry*. 2012;84:102–115. doi:10.1016/j.phytochem.2012.07.020
25. Izumi Y, Sawada H, Sakka N, et al. p-quinone mediates 6-hydroxydopamine-induced dopaminergic neuronal death and ferrous iron accelerates the conversion of p-quinone into melanin extracellularly. *J Neurosci Res*. 2005;79(6):849–860. doi:10.1002/jnr.20382
26. Agarwal S, Muqit MMK. PTEN-induced kinase 1 (PINK1) and Parkin: Unlocking a mitochondrial quality control pathway linked to Parkinson's disease. *Curr Opin Neurobiol*. 2022;72:111–119. doi:10.1016/j.conb.2021.09.005
27. Glinka Y, Gassen M, Youdim MBH. Mechanism of 6-hydroxydopamine neurotoxicity. In: Riederer P, Calne DB, Horowski R, Mizuno Y, Poewe W, Youdim MBH editors. *Advances in Research on Neurodegeneration. Journal of Neural Transmission. Supplementa*. Springer; 1997:55–66. doi:10.1007/978-3-7091-6842-4_7.
28. Soto-Otero R, Méndez-álvarez E, Hermida-Ameijeiras Á, Muñoz-Patiño AM, Labandeira-Garcia JL. Autoxidation and neurotoxicity of 6-Hydroxydopamine in the presence of some antioxidants. *J Neurochem*. 2000;74(4):1605–1612. doi:10.1046/j.1471-4159.2000.0741605.x
29. Lehrich BM, Liang Y, Fiandaca MS. Foetal bovine serum influence on in vitro extracellular vesicle analyses. *J Extracell Vesicles*. 2021;10(3):e12061. doi:10.1002/jev2.12061
30. Umar T, Shalini S, Raza MK, et al. New amyloid beta-disaggregating agents: Synthesis, pharmacological evaluation, crystal structure and molecular docking of N-(4-((7-chloroquinolin-4-yl)oxy)-3-ethoxybenzyl)amines. *MedChemComm*. 2018;9(11):1891–1904. doi:10.1039/C8MD00312B
31. Sharifi-Rad M, Ozcelik B, Altın G, et al. Salvia spp. Plants-from farm to food applications and phytopharmacotherapy. *Trends Food Sci Technol*. 2018;80:242–263. doi:10.1016/j.tifs.2018.08.008
32. Al-Qudah TS, Shibli RA, Zatimeh A, Tahtamouni RW, Al-Zyoud F. A sustainable approach to in vitro propagation and conservation of Salvia Dominica L.: A wild medicinal plant from *Jordan*. *Sustainability*. 2023;15(19):14218. doi:10.3390/su151914218
33. Yugay Y, Tsydeneshieva Z, Rusapetova T, et al. Isolation and characterization of extracellular vesicles from Arabidopsis *thaliana* cell culture and investigation of the specificities of their biogenesis. *Plants*. 2023;12(20):3604. doi:10.3390/plants12203604
34. Woith E, Guerriero G, Hausman JF, et al. Plant extracellular vesicles and nanovesicles: Focus on secondary metabolites, proteins and lipids with perspectives on their potential and sources. *Int J Mol Sci*. 2021;22(7):3719. doi:10.3390/ijms22073719
35. De Palma M, Ambrosone A, Leone A, et al. Plant roots release small extracellular vesicles with antifungal activity. *Plants*. 2020;9(12):1777. doi:10.3390/plants9121777
36. Visan KS, Lobb RJ, Ham S, et al. Comparative analysis of tangential flow filtration and ultracentrifugation, both combined with subsequent size exclusion chromatography, for the isolation of small extracellular vesicles. *J Extracell Vesicles*. 2022;11(9):e12266. doi:10.1002/jev2.12266
37. Rutter BD, Innes RW. Extracellular vesicles as key mediators of plant–microbe interactions. *Curr Opin Plant Biol*. 2018;44:16–22. doi:10.1016/j.pbi.2018.01.008
38. He B, Hamby R, Jin H. Plant extracellular vesicles: Trojan horses of cross-kingdom warfare. *FASEB BioAdvances*. 2021;3(9):657–664. doi:10.1096/fba.2021-00040
39. Pinedo M, de la CL, de M LC. A call for Rigor and standardization in plant extracellular vesicle research. *J Extracell Vesicles*. 2021;10(6):e12048. doi:10.1002/JEV2.12048
40. Wu YB, Ni ZY, Shi QW, et al. Constituents from Salvia species and their biological activities. *Chem Rev*. 2012;112(11):5967–6026. doi:10.1021/cr200058f
41. Kuźma Ł, Skrzypek Z, Wysokińska H. Diterpenoids and triterpenoids in hairy roots of Salvia sclarea. *Plant Cell Tissue Organ Cult*. 2006;84(2):171–179. doi:10.1007/s11240-005-9018-6
42. Alfieri M, Vaccaro MC, Cappetta E, Ambrosone A, De Tommasi N, Leone A. Coactivation of MEP-biosynthetic genes and accumulation of abietane diterpenes in Salvia sclarea by heterologous expression of WRKY and MYC2 transcription factors. *Sci Rep*. 2018;8(1). doi:10.1038/s41598-018-29389-4

43. Yadav VR, Prasad S, Sung B, Kannappan R, Aggarwal BB. Targeting inflammatory pathways by triterpenoids for prevention and treatment of cancer. *Toxins*. 2010;2(10):2428–2466. doi:10.3390/toxins2102428
44. Checker R, Sandur SK, Sharma D, et al. Potent anti-inflammatory activity of ursolic acid, a triterpenoid antioxidant, is mediated through suppression of NF-κB, AP-1 and NF-AT. *PLoS One*. 2012;7(2):e31318. doi:10.1371/journal.pone.0031318
45. Lehbili M, Alabdul Magid A, Kabouche A, et al. Antibacterial, antioxidant and cytotoxic activities of triterpenes and flavonoids from the aerial parts of Salvia barrelieri Etl. *Nat Prod Res*. 2018;32(22):2683–2691. doi:10.1080/14786419.2017.1378207
46. Poewe W, Seppi K, Tanner CM, et al. Parkinson disease. *Nat Rev Dis Primer*. 2017;3(1):1–21. doi:10.1038/nrdp.2017.13
47. Pinnell JR, Cui M, Tieu K. Exosomes in Parkinson disease. *J Neurochem*. 2021;157(3):413–428. doi:10.1111/jnc.15288
48. Emmanouilidou E, Melachroinou K, Roumeliotis T, et al. Cell-produced α-synuclein is secreted in a calcium-dependent manner by exosomes and impacts neuronal survival. *J Neurosci*. 2010;30(20):6838–6851. doi:10.1523/JNEUROSCI.5699-09.2010
49. Galindo MF, Saez-Atienzar S, Solesio ME, Jordán J. 6-Hydroxydopamine as preclinical model of parkinson's disease. In: Kostrzewa RM editor. *Handbook of Neurotoxicity*. Springer; 2014:639–651. doi:10.1007/978-1-4614-5836-4_5.
50. Ioghen OC, Ceafalan LC, Popescu BO. SH-SY5Y cell line in vitro models for Parkinson disease research-old practice for new trends. *J Integr Neurosci*. 2023;22(1):20. doi:10.31083/j.jin2201020
51. Henrich MT, Oertel WH, Surmeier DJ, Geibl FF. Mitochondrial dysfunction in Parkinson's disease – a key disease hallmark with therapeutic potential. *Mol Neurodegener*. 2023;18(1):83. doi:10.1186/s13024-023-00676-7
52. Dawson TM, Dawson VL. The role of parkin in familial and sporadic Parkinson's disease. *Mov Disord*. 2010;25(S1):S32–S39. doi:10.1002/mds.22798
53. Chen D, Zhang XY, Sun J, et al. Asiatic acid protects dopaminergic neurons from neuroinflammation by suppressing mitochondrial ros production. *Biomol Ther*. 2019;27(5):442–449. doi:10.4062/biomolther.2018.188
54. Ding H, Xiong Y, Sun J, Chen C, Gao J, Xu H. Asiatic acid prevents oxidative stress and apoptosis by inhibiting the translocation of α-synuclein into mitochondria. *Front Neurosci*. 2018;12. doi: 10.3389/fnins.2018.00431
55. Bang Y, Kwon Y, Kim M, Moon SH, Jung K, Choi HJ. Ursolic acid enhances autophagic clearance and ameliorates motor and non-motor symptoms in Parkinson's disease mice model. *Acta Pharmacol Sin*. 2023;44(4):752–765. doi:10.1038/s41401-022-00988-2
56. Peshattiwar V, Muke S, Kaikini A, Bagle S, Dighe V, Sathaye S. Mechanistic evaluation of Ursolic acid against rotenone induced Parkinson's disease– emphasizing the role of mitochondrial biogenesis. *Brain Res Bull*. 2020;160:150–161. doi:10.1016/j.brainresbull.2020.03.003
57. Bae HJ, Kim J, Kim J, et al. The effect of maslinic acid on cognitive dysfunction induced by cholinergic blockade in mice. *Br J Pharmacol*. 2020;177(14):3197–3209. doi:10.1111/bph.15042
58. Chen C, Ai Q, Shi A, Wang N, Wang L, Wei Y. Oleanolic acid and ursolic acid: Therapeutic potential in neurodegenerative diseases, neuropsychiatric diseases and other brain disorders. *Nutr Neurosci*. 2023;26(5):414–428. doi:10.1080/1028415X.2022.2051957
59. Msibi ZNP, Mabandla MV. Oleanolic acid mitigates 6-hydroxydopamine neurotoxicity by attenuating intracellular ROS in PC12 cells and striatal microglial activation in rat brains. *Front Physiol*. 2019;10:1059. doi:10.3389/fphys.2019.01059
60. Pingale TD, Gupta GL. Oleanolic acid-based therapeutics ameliorate rotenone-induced motor and depressive behaviors in parkinsonian male mice via controlling neuroinflammation and activating Nrf2-BDNF-dopaminergic signaling pathways. *Toxicol Mech Methods*. 2023;1–15. doi:10.1080/15376516.2023.2288198
61. Hanrott K, Gudmunsen L, O'Neill MJ, Wonnacott S. 6-hydroxydopamine-induced apoptosis is mediated via extracellular auto-oxidation and caspase 3-dependent activation of protein kinase Cdelta. *J Biol Chem*. 2006;281(9):5373–5382. doi:10.1074/jbc.M511560200